Summer 2013

Numerical Solutions to the Gross-Pitaevskii Equation for Bose-Einstein Condensates

Luigi Galati

NUMERICAL SOLUTIONS TO THE GROSS-PITAEVSKII EQUATION FOR BOSE-EINSTEIN CONDENSATES

by

LUIGI GALATI

(Under the Direction of Shijun Zheng)

ABSTRACT

In this thesis we compare various potential operators for the two-dimensional (2D) Gross-Pitaevskii equation (GPE) for Bose-Einstein condensates. Both the 2D and the 1D models are scaled to get a three parameter model. Smoothness of initial conditions is considered and choice of method (Split-Step Fourier method with Strang Splitting) is justified. Numerical simulations provide graphical evidence of properties of both focusing and nonfocusing cases.

Index Words: Bose-Einstein Condensation, Gross-Pitaevskii, mathematics, partial differential equations

2010 *Mathematics Subject Classification*: 65Z05, 65T50, 65M12

NUMERICAL SOLUTIONS TO THE GROSS-PITAEVSKII EQUATION FOR BOSE-EINSTEIN CONDENSATES

by

LUIGI GALATI

B.S., University of Florida

B.A., University of Florida

M.Ed, University of Florida

A Thesis Submitted to the Graduate Faculty of Georgia Southern University in Partial Fulfillment

of the Requirement for the Degree

MASTER OF SCIENCE

STATESBORO, GEORGIA

2013

NUMERICAL SOLUTIONS TO THE GROSS-PITAEVSKII EQUATION FOR BOSE-EINSTEIN CONDENSATES

by

LUIGI GALATI

Major Professor: Shijun Zheng

Committee: Yan Wu

Cheng Zhang

Electronic Version Approved:

July, 2013

DEDICATION

This thesis is dedicated to my wife Lacy who probably has done more to teach me how to think than anyone I know.

ACKNOWLEDGMENTS

I wish to acknowledge my committee members, Dr. Zheng, Dr. Wu, and Dr. Zhang. Countless hours were spent in Dr. Zheng's office just talking about physics and how we could harness it with the mathematics of partial differential equations. Dr. Wu was a great help in coding, and also with elements of analysis from previous courses. Dr. Zheng brought his expertise in partial differential equation. I also wish to acknowledge my classmates, especially those who graduated a semester or two earlier than me. I needed the push.

TABLE OF CONTENTS

LIST OF TABLES

Table Page

LIST OF FIGURES

Figure Page

LIST OF SYMBOLS

$\mathbb{R}$	the set of all real numbers
$\mathbb{R}^n$	n-dimensional real Euclidean space
$\mathbb{C}$	the set of all complex numbers
$\mathbb{N}$	the set of all natural numbers
$\sum$	sum
C^∞	the set of all functions with infinitely many conti nuous derivatives
$\prod$	product
$\mathbf{p}$	momentum
$\hbar$	Planck's constant
∇	gradient
Ψ	system wave function
ϕ	single particle wave function
ψ	condensation single particle wave function
$\mathbf{r}$	position vector
Δ	Laplacian operator
$\omega_x, \omega_y, \omega_z$	frequency in the x, y, z directions respectively
H	Hamiltonian
E	Energy
u_x	partial derivative of u with respect to x
u_{xx}, u_{xy}	second partial derivative of u w.r.t. x, partial x partial$y$
$\widehat{U}$	Fourier transform of U
$\psi*$	complex conjugate of ψ
$\|u(x)\|_{L^2}$	L^2 function norm
$\|\mathbf{u}\|_{\mathbf{l^2}}$	discrete l^2 vector norm
$f(x) = \mathcal{O}(g(x))$	there exists a positive real number M and a re al number x_0 such that $\|f(x)\| \leq M\|g(x)\|$ for all $x > x_0$
H^s	Sobolev space
$[A, B]$	commutator
Δt	step size
Δx	grid size in x direction
h	generic grid size
x_j	jth grid point
t^n	time level $n\Delta t$

U_j^n	numerical approximation of $v(x,t)$ at grid point x_j and time level t^n
$\frac{d^n}{dx^n}$	nth derivative
$\frac{\partial^n}{\partial x^n}$	nth partial derivative
a	scattering length

CHAPTER 1

INTRODUCTION

1.1 Brief History of Bose-Einstein Condensation

In 1924, Satyendra Nath Bose published a paper describing the statistical nature of light [7]. Using Bose's paper, Albert Einstein predicted a phase transition in a gas of noninteracting atoms could occur due to these quantum statistical effects. This phase transition period, Bose-Einsten Condensation, would allow for a macroscopic number of non-interacting bosons to simultaneously occupy the same quantum state of lowest energy [9].

It wasn't until 1938, with the discovery of superfluidity in liquid helium, that F. London conjectured that this superfluidity may be one of the first manifestations of BEC [13]. The real breakthrough came in 1995, when the Anderson group out of the University of Colorado produced a Bose-Einstein condensate from a vapor of rubidium atoms [2]. Their apparatus used a magnetic trap along with evaporative cooling. Just four months later, Davis of the Massachusetts Institute of Technology was able to produce the condensate from sodium atoms through the use of a similar scheme [8]. In each of these experiments, the magnetic trap confined the atoms cooling them down to a scale of microkelvins when velocity-distribution measurements gave the first indications of the Bose-Einstein condensation. Once the magnetic trap was turned of, the atoms expanded and then were optically cooled, producing the signature spike in velocity of the condensate. For their work, Cornell and Wieman out of Colorado and Ketterle of MIT were awarded the Nobel Prize in Physics.

The Gross-Pitaevskii equation (GPE), a nonlinear Schrödinger equation (NLSE) for the macroscopic wave functions, governs the properties of a BEC at temperatures T far below the critical condensation temperature T_c. The GPE includes a term for the trap potential as well as the mean field interaction between atoms in the gas which

manifests as a nonlinear term. Attractive interactions as well as repulsive interactions are accounted for in the GPE through the use of a focussing constant which may be positive (focussing) or negative (defocussing).

Numerical methods for solving the GPE are not new. Most methods involve discretizing spacial dimensions and then advancing via a time step. Spectral and pseudo-spectral methods were achieved by Bao, Jaksch, and Markowich [3], Bao and Shen [5]. Ruprecht et. al [17] proposed a Crank-Nicholson method in 1995 (the same year the first condensates were discovered.) Convergence analysis of these numerical methods, however, is relatively new.

1.2 The Organization of the thesis

The thesis is organized as follows:

In Chapter 2, the time dependent Gross-Pitaevskii Equation is formally introduced and derived. The GPE is converted into the dimensionless version through introduction of three parameters.

In Chapter 3, the numerical methods the split step methods Lie Splitting and Strang splitting are introduced. Stability and error parameters for the Lie Splitting are proved for the linear Schrödinger equation based on [3] and [4]. Lubich's error estimates [14] for GPE (cubic NLS) are then provided, but not proven.

Chapter 4 presents numerical illustrations of the error estimates of Chapter 3 as well as illustrations of the focusing effects of the BEC under certain conditions. Several different harmonic potentials are provided as examples of the interaction between attractive/repulsive potentials in addition to attractive/repulsive nonlinearities.

The final chapter serves as a conclusion with reference to potential future work.

CHAPTER 2

GROSS-PITAEVSKII EQUATION

First we derive the time independent Gross-Pitaevskii equation based on [16]. Recall that effective interaction between two particles (here we are looking at bosons) at a low energy is $U_0 = 4\pi\hbar^2 a/m$ which corresponds to a contact interaction of $U_0\delta(\mathbf{r}-\mathbf{r}')$ with $\mathbf{r}$ and $\mathbf{r}'$ being the locations of the two particles. Due to the inherent complications in dealing with a many-bodied system, a mean-field approach is used. At ultra low temperatures, all bosons exist in the same single-particle state $\phi(\mathbf{r})$ and for this reason we can write the wave function of the N-particle system as

$$\Psi(\mathbf{r}_1, \mathbf{r}_2, \ldots, \mathbf{r}_N) = \prod_{i=1}^{N} \phi(\mathbf{r}_i). \tag{2.1}$$

with $\Psi : \mathbb{R}^{n\times N} \to \mathbb{R}$ and $\phi : \mathbb{R}^n \to \mathbb{R}$. The single-particle wave function $\phi(\mathbf{r})$ obeys the typical normalization condition:

$$\int_{\mathbb{R}^3} |\phi(\mathbf{r})|^2 d\mathbf{r} = 1 \tag{2.2}$$

Due to the fact that we are dealing with dilute gases, the distances between the particles is such that the only interaction term is the $U_0\delta(\mathbf{r}-\mathbf{r}')$ mentioned earlier. Any other interactions are not accounted for in the mean-field theory. Thus the Hamiltonian can be written as follows:

$$H = \sum_{i=1}^{N} \left[\frac{\mathbf{p}_i^2}{2m} + V(\mathbf{r}_i)\right] + U_0 \sum_{i<j} \delta(\mathbf{r}-\mathbf{r}') \tag{2.3}$$

with $V(\mathbf{r})$ the external potential. The state (2.1) has energy

$$E = N \int \left[\frac{\hbar^2}{2m}|\nabla\phi(\mathbf{r})|^2 + V(\mathbf{r})|\phi(\mathbf{r})|^2 + \frac{(N-1)}{2}U_0|\phi(\mathbf{r})|^4\right] d\mathbf{r} \tag{2.4}$$

where $U_0 = \frac{4\pi\hbar^2 a}{m}$ (a is the scattering length) is the effective interaction between particles.

Though the Hartree approximation considers all atoms in the BEC gas to be in the state ϕ, in reality only a proportion of the total number are in this state due to interactions between the atoms. The reduced particle density in the BEC state governed by the GPE (Gross-Pitaevskii Equation) can be shown to be [16]

$$n = \frac{1}{(4\pi/3)r_s^3}. \tag{2.5}$$

Here, r_s is the radius of the sphere having an equal volume to the that of the average volume per particle.

Consider a uniform Bose gas in a volume V. In this system, the ground state wave function would be $1/V^{1/2}$ and thus the interaction energy for a pair of particles is U_0/V. Since all possible pairs of interactions between particles is $N(N-1)/2$, the energy becomes (with $N \gg 1$):

$$E = \frac{N(N-1)}{2V}U_0 \approx \frac{1}{2}Vn^2U_0 \tag{2.6}$$

where $n = N/V$. Here we introduce the wave function for the condensed state:

$$\psi(\mathbf{r}) = N^{1/2}\phi(\mathbf{r}) \tag{2.7}$$

and the density of particles is

$$n(\mathbf{r}) = |\psi(\mathbf{r})|^2. \tag{2.8}$$

This gives the energy of the particles in the condensed state as

$$E(\psi) = \int \left[\frac{\hbar^2}{2m}|\nabla\psi(\mathbf{r})|^2 + V(\mathbf{r})|\psi(\mathbf{r})|^2 + \frac{1}{2}U_0|\psi(\mathbf{r})|^4\right] d\mathbf{r} \tag{2.9}$$

The following condition of particle number conservation

$$N = \int |\psi|^2 d\mathbf{r} = \text{constant} \tag{2.10}$$

will be used in the last step. Finally we use the method of Lagrange multipliers where we take $\delta E = \mu\delta N = 0$. The Lagrange multiplier μ guarantees that the number of

particles remains constant and variations of ψ and $\psi*$ are arbitrary. The variation of $E - \mu N$ is then set equal to zero with respect to $\psi * (\mathbf{r})$ gives us

$$-\frac{\hbar^2}{2m}\nabla^2\psi(\mathbf{r}) + V(\mathbf{r})\psi(\mathbf{r}) + U_0|\psi(\mathbf{r})|^2\psi(\mathbf{r}) = \mu\psi(\mathbf{r}) \tag{2.11}$$

which is the time-independent Gross-Pitaevskii equation. Essentially the GPE is a Schrödinger equation with a total potential energy consisting of an external potential $V(\mathbf{r})$ and also the additional nonlinear term $U_0|\psi(\mathbf{r})|^2$ which represents the mean field produced by the interaction between the bosons.

2.1 Dimensionless Gross-Pitaevskii Equation

For the purposes of this thesis, we will use the following form of the GPE which has a harmonic trap potential, $V(\mathbf{x})$:

$$i\hbar\frac{\partial\psi(\mathbf{x},t)}{\partial t} = -\frac{\hbar^2}{2m}\nabla^2\psi(\mathbf{x},t) + \frac{m}{2}\left(\omega_x^2x^2 + \omega_y^2y^2 + \omega_z^2z^2\right)\psi(\mathbf{x},t) + NU_0|\psi(\mathbf{x},t)|^2\psi(\mathbf{x},t) \tag{2.12}$$

To scale the GPE with harmonic trap (2.12) with the normalization condition from earlier (2.2), the following parameters are introduced [3]:

$$\tilde{t} = \omega_x t, \quad \tilde{\mathbf{x}} = \frac{\mathbf{x}}{x_x}, \quad \tilde{\psi}(\tilde{\mathbf{x}},\tilde{t}) = x_s^{3/2}\psi(\mathbf{x},t). \tag{2.13}$$

We consider x_s to be the characteristic 'length' of the condensate. Combining (2.13) with (2.12), multiplying by $\frac{1}{m\omega_x^2 x_s^{1/2}}$ and removing all $\tilde{}$, the dimensionless GPD is as follows:

$$i\varepsilon\frac{\partial\psi(\mathbf{x},t)}{\partial t} = -\frac{\varepsilon^2}{2}\nabla^2\psi(\mathbf{x},t) + V(\mathbf{x})\psi(\mathbf{x},t) + \delta\varepsilon^{5/2}|\psi(\mathbf{x},t)|^2\psi(\mathbf{x},t) \tag{2.14}$$

where

$$\begin{aligned} V(\mathbf{x}) &= \frac{1}{2}\left(x^2 + \gamma_y^2y^2 + \gamma_z^2z^2\right), \\ \varepsilon &= \frac{\hbar}{\omega_x m x_s^2} = \left(\frac{a_0}{x_s}\right)^2, \quad \gamma_y = \frac{\omega_y}{\omega_x}, \quad \gamma_z = \frac{\omega_z}{\omega_x} \\ \delta &= \frac{U_0N}{a_o^3\hbar\omega_x} = \frac{4\pi aN}{a_0}, \quad a_0 = \sqrt{\frac{\hbar}{\omega_x m}} \end{aligned} \tag{2.15}$$

Here, a_0 is the x-direction length of the harmonic oscillator ground state, γ_y, γ_z are simply the ratios of the magnitudes of the frequency of the oscillator in the y-direction and z-direction relative to the frequency in the x-direction. $\delta\varepsilon^{5/2}$ can be rewritten and defined in the following way:

$$\kappa := \frac{4\pi aN}{a_0}\left(\frac{a_0}{x_s}\right)^5 = \frac{1}{2}\frac{8\pi aN}{x_s^3}\frac{a_0^4}{x_s^2} = \frac{\mathrm{sgn}(a)}{2}\frac{a_0^2}{x_h^2}\frac{a_0^2}{x_s^2} = \frac{\mathrm{sgn}(a)}{2}\left(\frac{a_0}{x_h}\frac{a_0^2}{x_s}\right)^2 \tag{2.16}$$

with x_h defined as the healing length [6]:

$$x_h := \left(\frac{8\pi|a|N}{x_s^3}\right)^{-1/2} \tag{2.17}$$

2.2 Choice of Parameters

Given the previous definitions, the parameters ε and κ have special meaning. The level of interaction in the condensate can be measured by these parameters. In the case where $x_s = a_0$ (the characteristic length of the condensate is the same as the length of the harmonic oscillator ground state) then $\varepsilon = 1$ by (2.14), and $\kappa = \delta$ by (2.16). This combination of parameters is typical in the weak interaction regime ($4\pi|a|N \ll a_0$) and the moderate interaction regime ($4\pi|a|N \approx a_0$). The strong interaction regime ($4\pi|a|N \gg a_0$) might find a possible choice of parameters such as [3] $x_s = (4\pi|a|Na_0^4)^{1/5}$, giving $|\kappa| = 1$ and $\varepsilon = \left(\frac{a_0}{4\pi|a|N}\right)^{1/5} \ll 1$.

This gives us two extreme regimes, $\varepsilon = \mathcal{O}(1)$ which implies that $a_0 = \mathcal{O}(x_s)$ and $\kappa = \delta\varepsilon^{5/2} = o(1)$ which implies that $4\pi|a|N \ll a_0$ which puts the interactions in the weak regime and $\varepsilon = o(1)$ which implies that $x_s \gg a_0$ and $\kappa = \delta\varepsilon^{5/2} = \mathcal{O}(1)$ which implies that $4\pi|a|N \gg a_0$ (in the case of our dimensionless GPE, $\varepsilon = 1$ and $\kappa = \delta\varepsilon^{5/2} = \delta$ where $\delta \gg 1$). In this thesis, we will be selecting $\varepsilon = 1$ with $\kappa = 1$ (defocusing case) as well as $\varepsilon = 0.3$ with $\kappa = -1.9718$.

2.3 General Strang Splitting

In this section we describe the splitting method first arrived at by Strang in 1968 [18]. This section will begin by being based on the linear hyperbolic model problem

$$u_t = Au_x + Bu_y \tag{2.18}$$

with A, B as operators which may be represented as matrices. In order to comment on the accuracy of difference schemes in this section we will be using the following notation:

$$U(t+k,k) = S_k U(t,k). \tag{2.19}$$

Typically we use a weighted sum to calculate S_k

$$(S_k f)(x,y) = \sum C_{ij} f(x+ih, y+jh). \tag{2.20}$$

The order of accuracy is determined by comparing the difference operator $S_k u$ to the Taylor expansion of $u(t+k)$ as follows:

$$S_k u = u + ku_t + \frac{k^2}{2}u_{tt} + O(k^3) \tag{2.21}$$

Using this expansion and the hyperbolic differential equation, we wish to achieve second order accuracy by fulfilling the following condition

$$S_k f \approx f + k(Af_x + Bf_y) + \frac{k^2}{2}(A^2 f_{xx} + (AB+BA)f_{xy} + B^2 f_{yy}) \tag{2.22}$$

with $\approx$ indicating equality up to $O(k^3)$. We define the Lax-Wendroff operator for one space variable ($B = 0$):

$$L_k^x = I + rA\Delta_0 \frac{r^2}{2} A^2 \Delta_{+-} \tag{2.23}$$

which was first arrived at in [12] and is second order accurate given

$$\Delta_0 = \frac{1}{2}(f(x+h) - f(x-h)) \approx hf_x(x),$$

$$\Delta_{x-} f(x) = f(x+h) - 2f(x) + f(x-h) \approx h^2 f_{xx}(x).$$

Stability in this section is tested by first applying the difference operator to exponentials:

$$\begin{aligned} L_k^x e^{i\xi x} v &= \left(I + irA\sin(\xi h) + \frac{r^2}{2} A^2 (1 - cos(\xi h)) \right) e^{i\xi x} v \\ &= G_x(\xi h) e^{i\xi x} v \end{aligned}$$

then testing that the amplification matrices G have uniformly bounded powers:

$$|(G_x(\xi h))^n v| \leqq \text{ const. } |v| \tag{2.24}$$

for all real ξh, all $n > 0$ and all vectors v. Another stability condition requires the eigenvalues of the operator A of the Lax-Wendroff operator L_k^x satisfy

$$\max |\lambda_j(A)| \leqq \frac{h}{k} = \frac{1}{r} \tag{2.25}$$

and thus implying L_k^x dissipates energy:

$$\int |L_k^x f(x)|^2 dx \leqq \int |f(x)|^2 dx.$$

The Strang Splitting method begins with the introduction of

$$S_k^{(5)} = L_{k/2}^x L_k^y L_{k/2}^x \tag{2.26}$$

where

$$L_{k/2}^x = I + \frac{k}{2h} A \Delta_0^x + \frac{1}{2} \left(\frac{k}{2h} \right)^2 A^2 \Delta_{+-}^x.$$

Note that the operator $L_{k/2}^x$ is strongly stable so long as $|\lambda_j(A)| \leqq 2h/k$ and L_k^y is strongly stable so long as $|\mu_j(B)| \leqq 2h/k$. Together, these two conditions met simultaneously ensure that $S_k^{(5)}$ is also stable. This splitting (2.26) is second order accurate since

$$\begin{aligned} S_k^{(5)} &\approx \left(I + \frac{k}{2} A\partial_x + \frac{k^2}{8} A^2 \partial_x^2 \right) \left(I + kB\partial_y + \frac{k^2}{2} B^2 \partial_y^2 \right) \left(I + \frac{k}{2} A\partial_x + \frac{k^2}{8} A^2 \partial_x^2 \right) f \\ &\approx f + k(Af_x + Bf_y) + \frac{k^2}{2} (A^2 f_{xx} + (AB + BA) f_{xy} + B^2 f_y y) \end{aligned}$$

which is the condition previously mentioned (2.22). In the nonlinear case, notation is introduced for a general system:

$$u_t = c(D^\alpha u, \mathbf{x}, t) = a(D^\alpha u, \mathbf{x}, t) + b(D^\alpha u, \mathbf{x}, t).$$

Here, the splitting $c = a + b$ is arbitrary. $D^\alpha u$ runs over all derivatives (mixed or not) of the vector u with respect to the spatial variable $\mathbf{x} = (x_1, x_2, \ldots, x_d)$. This splitting gives us the following two (potentially) nonlinear problems

$$v_t = a(D^\alpha u, \mathbf{x}, t), \quad w_t = b(D^\alpha u, \mathbf{x}, t).$$

We refer to the difference operators for v_t and w_t as $M_k(t)$ and $N_k(t)$ respectively. Both $M_k(t)$ and $N_k(t)$ are of second order accuracy. To show this, (in the case of $N_k(t)$) w_t is differentiated and then each D^α is commuted with $\partial/\partial t$:

$$\begin{aligned} w_{tt} &= \sum_\alpha B_\alpha \frac{\partial}{\partial t}(D^\alpha w) + b_t \\ &= \sum_\alpha B_\alpha D^\alpha [b(D^\alpha w, \mathbf{x}, t)] + b_t(D^\alpha w, \mathbf{x}, t) \end{aligned}$$

where $B_\alpha = B_\alpha b(D^\alpha w, \mathbf{x}, t)$ is the Jacobian of b with respect to $D^\alpha w$. Now all that is necessary for $N_k(t)$ is that for any smooth vector function $f = f(x)$,

$$N_k(t) f \approx f + kb + \frac{k^2}{2}\left(\sum_\alpha B_\alpha D^\alpha [b(D^\alpha f, \mathbf{x}, t)] + b_t\right) \tag{2.27}$$

with b, b_t, B_α evaluated at $(D^\alpha f, \mathbf{x}, t)$.

Next the composite operator $S_k(t)$ is defined as follows:

$$S_k(t) = M_{k/2}\left(t + \frac{k}{2}\right) N_k(t) M_{k/2}(t)$$

Its accuracy is now verified using (2.27)

$$\begin{aligned} g = N_k(t)M_{k/2}(t)f &\approx M_{k/2}fkb(D^\alpha M_{k/2}f, \mathbf{x}, t) \\ &\quad + \frac{k^2}{2}\left(\sum B_\alpha D^\alpha [b(D^\alpha M_{k/2}f, \mathbf{x}, t)] + b_t\right) \\ &\approx f + \frac{k}{2}a + \frac{k^2}{8}\left(\sum A_\alpha D^\alpha a + a_t\right) \\ &\quad + k\left(b + \sum B_\alpha \frac{k}{2} D^\alpha a\right) + \frac{k^2}{8}\left(\sum B_\alpha D^\alpha b + b_t\right) \end{aligned} \tag{2.28}$$

Now we apply $M_{k/2}(t)$ to this vector to get:

$$\begin{aligned} S_k(t)f &\approx g + \frac{k}{2}a\left(D^\alpha g, \mathbf{x}, t + \frac{k}{2}\right) + \frac{k^2}{8}\left(\sum A_\alpha D^\alpha a + a_t\right) \\ &\approx g + \frac{k}{2}\left[a + \sum A_\alpha \left(\frac{k}{2}D^\alpha a + kD^\alpha b\right) + \frac{k}{2}a_t\right] \\ &\quad + \frac{k^2}{8}\left(\sum A_\alpha D^\alpha a + a_t\right) \\ &\approx f + k(a+b) + \frac{k^2}{8}\left[\sum (A_\alpha + B_\alpha)D^\alpha (a+b) + (a+b)_t\right]. \end{aligned} \tag{2.29}$$

Thus we have established the second order of accuracy of $S_k(t)$ which was the Strang Splitting in the nonlinear case.

CHAPTER 3

NUMERICAL METHOD

3.1 Numerical Method

In this section we present time-splitting trigonometric spectral approximations of the problem, with periodic boundary conditions. The first sections, 3.1 - 3.6, will be proofs of stability and error estimates in the linear case. The sections that follow are error estimates from Lubich [14] for the Strang Splitting method in the nonlinear case but without proof. The chapter concludes with a proof from For the simplicity of notation we shall introduce the method for the case of one space dimension ($d = 1$). The analysis in the next section will also focus on the case $d = 1$. Generalizations to $d > 1$ are straightforward for tensor product grids and the results remain valid without modifications. For $d = 1$, the problem becomes (with harmonic potential $V(x)$ and taking $\varepsilon = 1$):

$$iu_t = -\frac{u_{xx}(x,t)}{2} + \frac{x^2}{2}u(x,t) + \kappa_1|u(x,t)|^2u(x,t),\ a < x < b, \tag{3.1}$$

$$u(x, t = 0) = u^0(x),\ a \le x \le b, \tag{3.2}$$

$$u(a,t) = u(b,t),\ u_x(a,t) = u_x(b,t),\ t > 0 \tag{3.3}$$

Since the Schrödinger equation is time reversible, we let $t \in \mathbb{R}$ for Eqs. (3.1) and (3.2).

Spatial mesh size chosen is $h = \Delta x > 0$ with $h = (b-a)/M$ for M an even positive integer and the time step $k = \Delta t > 0$, and we let the grid points and the time step be

$$x_j := a + jh,\ t_n := nk,\ j = 0, 1, \ldots, M,\ n = 0, 1, 2, \ldots,$$

Let U_j^n be the approximation of $u(x_j, t_n)$ and $\mathbf{u}^n$ be the solution vector at time $t = t_n = nk$ with components u_j^n.

3.2 Lie Splitting Method (LS)

From time $t = t_n$ to time $t = t_{n+1}$, the Schrödinger equation (3.1) is solved in two steps. One first solves:

$$iu_t = -\frac{u_{xx}}{2} \tag{3.4}$$

for one step, followed by solving

$$iu_t = \frac{x^2}{2}u(x,t) + \kappa_1|u(x,t)|^2u(x,t), \tag{3.5}$$

again for one time step. Equation (3.4) is discretized in space by the spectral method and will be integrated in time exactly. Equation (3.5) is simply an ODE that can be solved exactly. The splitting method is completed as follows:

$$\begin{gathered}\widehat{U}_j^* = \frac{1}{M}\sum_{l=-M/2}^{M/2-1} e^{-ik\mu_l^2/2}\widehat{U}_l^n e^{i\mu_l(x_j-a)},\ j = 0,1,2,\ldots,M-1 \\ U_n^{n+1} = e^{-iV(x_j)k}U_j^*\end{gathered} \tag{3.6}$$

where $\widehat{U}_j^*$, the Fourier coefficients of U^n, are defined as

$$\mu_l = \frac{2\pi l}{b-a}, \quad \widehat{U}_l^n = \sum_{j=0}^{M-1} U_j^n e^{-i\mu_l(x_j-1)}, \quad l = \frac{M}{2},\ldots,\frac{M}{2}-1 \tag{3.7}$$

with

$$U_j^0 = u(x_j,0) = u_0(x_j), \quad j = 0,1,2,\ldots,M. \tag{3.8}$$

For this method, it is important to note that the only time discretization error of this method is the splitting error which is first order in k. For later proofs, we define the trigonometric interpolant of a function f on the grid $\{x_0, x_1, \ldots, x_M\}$:

$$f_l(x) = \frac{1}{M}\sum_{l=-M/2}^{M/2-1} \widehat{f}_l^* e^{i\mu_l(x_j-a)}, \quad \widehat{f} = \sum_{j=0}^{M-1} f(x_j)e^{-i\mu_l(x_j-1)}, \quad j = -\frac{M}{2},\ldots,\frac{M}{2} \tag{3.9}$$

3.3 The Strang Splitting Spectral Method (SS)

As in the previous method, eqn (3.1) will be split into two parts. This time, from time $t = t_n$ to $t = t_{n+1}$, we combine the splitting steps via the standard Strang splitting:

$$\begin{aligned} U_j^* &= e^{-i(V(x))k/2} U_j^n, \\ U_j^{**} &= \frac{1}{M} \sum_{l=-M/2}^{M/2-1} e^{-ik\mu_l^2/2} \widehat{U}_l^* e^{i\mu_l(x_j-a)}, \qquad j = 0, 1, 2, \ldots, M-1 \\ U_j^{n+1} &= e^{-i(x_j^2/2+\kappa_1|U_j^{**}|^2)k/2} U_j^{**} \qquad j = 0, 1, 2, \ldots, M-1 \end{aligned} \tag{3.10}$$

where $\widehat{U}_l^*$, the Fourier coefficients of U^*, are defined as

$$\widehat{U}_l^* = \sum_{j=0}^{M-1} U_j^* e^{-i\mu_l(x_j-1)}, \quad l = \frac{M}{2}, \ldots, \frac{M}{2} - 1 \tag{3.11}$$

The overall time discretization error comes solely from the splitting, which is second order in k. If $V(x) \equiv V =$ constant, then we can combine all time steps in both the Lie Splitting method and the Strang Splitting method into one method,

$$U_j^n = \frac{1}{M} \sum_{l=-M/2}^{M/2-1} e^{-i(\mu_l^2/2+V)t_n} \widehat{U}_l^0 e^{i\mu_l(x_j-a)} \tag{3.12}$$

where

$$\widehat{U}_l^0 = \sum_{j=0}^{M-1} U_j^0 e^{-i\mu_l(x_j-1)}, \quad l = \frac{M}{2}, \ldots, \frac{M}{2} - 1 \tag{3.13}$$

This is the same as descretizing the second order speace derivative in (3.1) by the spectral method, then solving the ODE system that results exactly to $t = t_n$. In this case, no time discretization error is introduced. The only error is the spectral error in the spatial derivative.

3.4 Error Estimates

First, stability of both methods, Lie Splitting and Strang Splitting, is proven. Then an estimate for the Lie Splitting method is provided and proved. Finally, an error

estimate is provided for the Strang Splitting method, however proof is withhold for brevity purposes. Let $\mathbf{u} = (u_0, \ldots, u_{M-1})^T$. Let $\| \times \|_{L^2}$ and $\| \times \|_{l^2}$ be the L^2-norm and the usual discrete l^2-norm respectively on the interval (a, b); i.e.,

$$\|u\|_{L^2} = \sqrt{\int_a^b |u(x)|^2 \, dx}, \ \|\mathbf{u}\|_{l^2} = \sqrt{\frac{b-a}{M} \sum_{j=0}^{M-1} |U_j|^2}. \tag{3.14}$$

For the *stability* of the Lie Splitting and Strang Splitting methods, with variable potential $V(x)$ we prove the following lemma, which shows that the total charge is conserved.

Lemma 3.4.1. *The time-splitting spectral schemes LS and SS are unconditionally stable. In fact,under any mesh size h and time step k,*

$$\|\mathbf{u}^n\|_{l^2} = \|u_0\|_{l^2} \quad n = 1, 2, \ldots, \tag{3.15}$$

and consequently

$$\|u_I^n\|_{L^2} = \|u_I^0\|_{L^2} \ n = 1, 2, \ldots, \tag{3.16}$$

Here, u_l^n stands for the trigonometric polynomial interpolating $\{(x_0, u_0^n), (x_1, u_1^n), \ldots, (x_M, u_M^n)\}$.

Proof. First let us recall the following identities:

$$\sum_{j=0}^{M-1} e^{i2\pi(k-l)j/M} = \begin{cases} 0 & k - l \neq mM, \\ M & k - l = mM, \end{cases} \quad m \text{ integer} \tag{3.17}$$

and

$$\sum_{l=-M/2}^{M/2-1} e^{i2\pi(k-j)l/M} = \begin{cases} 0 & k - j \neq mM, \\ M & k - j = mM, \end{cases} \quad m \text{ integer.} \tag{3.18}$$

For the scheme LS (3.6), noting (3.7) and (3.14), we have:

$$\begin{aligned}
\frac{1}{b-a}\|\mathbf{u}^{n+1}\|_{l^2}^2 &= \frac{1}{M}\sum_{j=0}^{M-1}|U_j^{n+1}|^2 = \frac{1}{M}\sum_{j=0}^{M-1}|e^{-iV(x_j)k}U_j^*|^2 = \frac{1}{M}\sum_{j=0}^{M-1}|U_j^*|^2 \\
&= \frac{1}{M}\sum_{j=0}^{M-1}\left|\frac{1}{M}\sum_{l=-M/2}^{M/2-1} e^{-ik\mu_l^2/2}\widehat{U}_l^n e^{i\mu_l(x_j-a)}\right|^2 \\
&= \frac{1}{M^2}\sum_{l=-M/2}^{M/2-1}|e^{-ik\mu_l^2/2}\widehat{U}_l^n|^2 \\
&= \frac{1}{M^2}\sum_{l=-M/2}^{M/2-1}|\widehat{U}_l^n|^2 \\
&= \frac{1}{M^2}\sum_{l=-M/2}^{M/2-1}\left|\sum_{j=0}^{M-1} U_j^n e^{-i\mu_l(x_j-a)}\right|^2 \\
&= \frac{1}{M}\sum_{j=0}^{M-1}|U_j^n|^2 \\
&= \frac{1}{b-a}\|\mathbf{u}^n\|_{l^2}^2
\end{aligned} \tag{3.19}$$

Now, for the Strang Splitting scheme (3.10), using (3.11), (3.14) and the identities from above (3.17) and (3.18),

$$\begin{aligned}
\frac{1}{b-a}\|\mathbf{u}^{n+1}\|_{l^2}^2 &= \frac{1}{M}\sum_{j=0}^{M-1}|U_j^{n+1}|^2 = \frac{1}{M}\sum_{j=0}^{M-1}|e^{-iV(x_j)k/2}U_j^{**}|^2 = \frac{1}{M}\sum_{j=0}^{M-1}|U_j^{**}|^2 \\
&= \frac{1}{M}\sum_{j=0}^{M-1}\left|\frac{1}{M}\sum_{l=-M/2}^{M/2-1} e^{-ik\mu_l^2/2}\widehat{U}_l^* e^{i\mu_l(x_j-a)}\right|^2 \\
&= \frac{1}{M^2}\sum_{l=-M/2}^{M/2-1}|e^{-ik\mu_l^2/2}\widehat{U}_l^*|^2 \\
&= \frac{1}{M^2}\sum_{l=-M/2}^{M/2-1}|\widehat{U}_l^*|^2 \\
&= \frac{1}{M^2}\sum_{l=-M/2}^{M/2-1}\left|\sum_{j=0}^{M-1} U_j^* e^{-i\mu_l(x_j-a)}\right|^2 \\
&= \frac{1}{M}\sum_{j=0}^{M-1}|U_j^*|^2 \\
&= \frac{1}{M}\sum_{l=-M/2}^{M/2-1}|e^{-ik\mu_l^2/2}U_j^n|^2 \\
&= \frac{1}{M}\sum_{j=0}^{M-1}|U_j^n|^2 \\
&= \frac{1}{b-a}\|\mathbf{u}^n\|_{l^2}^2
\end{aligned} \tag{3.20}$$

Therefore, the stability condition (3.15) is proven from (3.19) for the Lie Splitting and for the Strang Splitting by induction, from (3.20). Finally it is important to note that for all periodic functions f, the following equality holds:

$$\|f_I\|_{L^2} = \|f\|_{l^2} = \sqrt{\frac{b-a}{M}\sum_{j=0}^{M-1}|f(x_j)|^2} \tag{3.21}$$

Here, f_I stands for the trigonometric interpolant of f on $\{x_0, x_1, \ldots, x_M\}$ that was defined earlier (3.9). Therefore, combining (3.21) with (3.15) we arrive at (3.16). □

In order to arrive at error estimates, it must be assumed that the initial condition u_0 in (3.1) is C^∞ on $\mathbb{R}$ and periodic with period $b-a$. Also, it is assumed that there

exist positive constants $C_m > 0$, for every integer $m \geq 0$, such that:

$$(A) \quad \left\| \frac{d^m}{dx^m} u_0 \right\|_{L^2(a,b)} \leq C_m, \quad \text{for all } m \in \mathbb{N} \cup \{0\} \tag{3.22}$$

The semiclassical WKB initial data

$$u(x,0) = \sqrt{n_0(x)} e^{iS_0(x)}$$

satisfies (3.22) so long as n_0 and S_0 are C^∞ on $\mathbb{R}$ and are $(b-a)$-periodic.

3.5 Error Analysis for Constant Potentials for Lie Splitting

For constant potential $V(x) \equiv V = \text{constant}$, both the Lie Splitting and the Strang Splitting reduce to (3.12).

Theorem 3.5.1. *Let u be the exact solution of (3.1), (3.2), let $V = \text{constant}$, and let u_I^N be the trigonometric interpolant of $\mathbf{u}^n = (U_j^n)_{j=0}^{M-1}$ as obtained from (3.12). Under assumption (A), we have for all integers $m \geq 1$*

$$\|u_I^n - u(t_n)\|_{L^2} \leq DC_m \left(\frac{h}{(b-a)} \right)^m, \tag{3.23}$$

where $D > 0$ is a constant.

Proof. From Theorem 3 in [15]the following estimate is concluded:

$$\|u_I^0 - u_0\|_{L^2} \leq D \left(\frac{h}{b-a} \right)^m \left\| \frac{d^m}{dx^m} u_0 \right\|_{L^2} \leq DC_m \left(\frac{h}{(b-a)} \right)^m, \tag{3.24}$$

for $m \geq 1$, where $D > 0$ depends only on $(b-a)$. Since u_I^n is the exact solution of (3.1) (subject to periodic boundary conditions) with u_I^0 as intial datum, at $t = t_n$, and since the Schrödinger equation generates a unitary group on the space $L^2(a,b)$, the estimate (3.23) follows. □

3.6 Error Analysis for Variable Potentials for Lie Splitting

In this section we provide error estimates for the Lie Splitting method for variable potential V. It is assumed that the solution $U = u(x,t)$ from (3.1) and (3.2) and the potential $V(x)$ in (3.1) are $C^\infty(\mathbb{R})$ and $(b-a)$-periodic. In addition, there exist positive constants $C_m > 0, D_m > 0$, independent of x, t such that

$$(B) \quad \left\| \frac{\partial^{m_1+m_2}}{\partial x^{m_1} \partial t^{m_2}} u \right\|_{C([0,T];L^2(a,b))} \leq C_{m_1+m_2}, \quad \left\| \frac{d^m}{dx^m} V \right\|_{L^\infty(a,b)} \leq D_m, \tag{3.25}$$
$$\text{for all } m, m_1, m_2 \in \mathbb{N} \cup \{0\}$$

These conditions imply that the solution oscillates in space and time. With this information we can prove the error estimate for the Lie Splitting in the case of a potential that is not constant, namely $V = V(x)$.

Theorem 3.6.1. *Let $u = u(x,t)$ be the exact solution of (3.1), (3.2) and $\mathbf{u}^n$ be the discrete approximation of the Lie Splitting method given by (3.6). Under assumption (B), and assumping $h, k = \mathcal{O}(1)$, we have for all positive integers $m \geq 1$ and $t_n \in [0,T]$ that*

$$\|u(t_n) - u_I^n\|_{L^2} \leq G_m \frac{T}{k} \left(\frac{h}{(b-a)} \right)^m + CTk \tag{3.26}$$

where C is a positive constant independent of h, k, and m and G_m is independent of h, k.

Proof. First, the local splitting error in (3.4) and (3.5) for (3.1) is estimated. The following operators will be used:

$$\mathcal{A} = \frac{ik}{2} \partial_{xx}, \quad \mathcal{B} = -iV(x)k \tag{3.27}$$

Let

$$w(x) = e^{\mathcal{B}} e^{\mathcal{A}} u(\cdot, t_n) \tag{3.28}$$

be the solution coming from the operator splitting method (without spatial discretization) after one time step with exact initial data at t_n. The exact solution $u(x, t_{n+1})$ is

$$u(x, t_{n+1}) = e^{\mathcal{B}+\mathcal{A}} u(\cdot, t_n) \tag{3.29}$$

and all error in this classical analysis comes from the non-commutativity of the operators $\mathcal{A}$ and $\mathcal{B}$ ($[\mathcal{A}, \mathcal{B}] \neq 0$). By (3.25)

$$\begin{aligned}(\mathcal{B}\mathcal{A} - \mathcal{A}\mathcal{B})u(x,t) &= \frac{k^2}{2}\partial_{xx}(Vu) - \frac{Vk^2}{2}\partial_{xx}u \\ &= \frac{k^2}{2}u\partial_x^2 V + k^2\partial_x V \partial_x u = \mathcal{O}(k^2)\end{aligned} \tag{3.30}$$

Now, if we perform a Taylor expansion of $e^{\mathcal{A}}, e^{\mathcal{B}}$ and $e^{\mathcal{A}+\mathcal{B}}$ we get

$$\|u(t_{n+1}) - w\|_{L^2} = \mathcal{O}(k^2) \tag{3.31}$$

This gives us

$$\|u(t_{n+1}) - u_I^{n+1}\|_{L^2} \leq \|u(t_{n+1}) - w\|_{L^2} + \|w - w_I\|_{L^2} + \|w_I - u_I^{n+1}\|_{L^2} \tag{3.32}$$

and

$$\begin{aligned}\|w_I - u_I^{n+1}\|_{L^2} &= \|w - u^{n+1}\|_{l^2} = \|e^{\mathcal{A}}(e^{\mathcal{B}}u(t_n) - e^{\mathcal{A}}u^n)\|_{l^2} \\ &= \|u(t_n) = u^n\|_{l^2} = \|u(t_n)_I - u_I^n\|_{L^2} \\ &\leq \|u(t_n)_I - u(t_n)\|_{L^2} + \|u(t_n) - u_I^n\|_{L^2}\end{aligned} \tag{3.33}$$

The first and fourth equalities use $\|f\|_{l^2} = \|f\|_{L^2}$. The second equality uses the definition of w and the fact that the computation of U_j^* in the first step in (3.6) is the same as the exact solution of the free Schrödinger equation (3.4) with u_I^n for initial data. The third equality comes from (3.15) (the conservation property). Therefore,

$$\begin{aligned}\|u(t_{n+1}) - u_I^{n+1}\|_{L^2} \leq \|u(t_{n+1}) - w\|_{L^2} + \|w - w_I\|_{L^2} + \|u(t_n)_I - u(t_n)\|_{L^2} \\ + \|u(t_n) - u_I^n\|_{L^2}\end{aligned} \tag{3.34}$$

From the proof of constant potential (3.24), we get

$$\|u(t_n)_I - u(t_n)\|_{L^2} \leq D\left(\frac{h}{b-a}\right)^m \left\|\frac{d^m}{dx^m}u(t_n)\right\|_{L^2} \leq DC_m\left(\frac{h}{(b-a)}\right)^m. \tag{3.35}$$

where Assumption (B) (3.25) was used. Similarly,

$$\|w - w_I\|_{L^2} \leq D\left(\frac{h}{b-a}\right)^m \left\|\frac{d^m}{dx^m}w\right\|_{L^2} \leq E_m\left(\frac{h}{(b-a)}\right)^m. \tag{3.36}$$

so long as $k, \frac{h}{b-a} = \mathcal{O}(1)$. Here we used

$$\begin{aligned}\left\|\frac{d^m}{dx^m}w\right\|_{L^2} &= \left\|\sum_{j=0}^{m}\binom{m}{j}(e^{\mathcal{B}})^{(j)}(e^{\mathcal{A}})u(t_n))^{(m-j)}\right\|_{L^2} \\ &\leq \sum_{j=0}^{m}\binom{m}{j}\|(e^{\mathcal{B}})^{(j)}\|_{L^\infty}\|(e^{\mathcal{A}})u(t_n))^{(m-j)}\|_{L^2}\end{aligned} \tag{3.37}$$

Finally, we use (3.31) to obtain

$$\|u(t_{n+1}) - u_I^{n+1}\|_{L^2} \leq Fk^2 + E_m\left(\frac{h}{(b-a)}\right)^m + DC_m\left(\frac{h}{(b-a)}\right)^m + \|u(t_n) - u_I^n\|_{L^2} \tag{3.38}$$

where again it is assumed that $k, \frac{h}{b-a} = \mathcal{O}(1)$. Then by induction, (3.26) follows. □

Thus we have proven the stability of both the Lie Splitting method and the Strang Splitting method. The error estimates for both methods have been proven for constant potentials $V(x) \equiv V =$ constant.

3.7 Convergence for H^4 Initial Conditions

The final section of this chapter is a presentation of convergence for initial condition $\psi_0 \in H^4$ presented by Lubich [14]. First, we introduce a shorthand notation for the Strang Splitting:

$$\begin{aligned}\psi_{n+1/2}^- &= e^{\frac{i}{2}\tau\Delta}\psi_n \\ \psi_{n+1/2}^+ &= e^{-i\tau V[\psi_{n+1/2}^-]}\psi_{n+1/2}^- \\ \psi_{n+1} &= e^{\frac{i}{2}\tau\Delta}\psi_{n+1/2}^+\end{aligned} \tag{3.39}$$

Next we suppose that the solution $\psi(t)$ to the cubic nonlinear Schrödinger equation (2.14) is in H^4 for $0 \leq t \leq T$, and set

$$m_4 = \max_{0 \leq t \leq T} \|\psi(t)\|_{H^4}$$

We will use the following

$$\psi_{n+1} = \Phi_r(\psi_n)$$

to represent a single step of the Strang Splitting.

The proofs of the following theorem and propositions will require the use of the following two lemmas and these will be presented without proof.

Lemma 3.7.1. *For $u \in H^1$ and $v, w \in L_2$,*

$$\|\Delta^{-1}(uv)w\|_{L_2} \leq K_0 \|u\|_{H^1} \|v\|_{L_2} \|w\|_{L_2} \tag{3.40}$$

and for $u, v \in L_2$ and $w \in H^1$,

$$\|\Delta^{-1}(uv)w\|_{L_2} \leq K_0 \|u\|_{L_2} \|v\|_{L_2} \|w\|_{H^1} \tag{3.41}$$

Lemma 3.7.2. *For $u, v, w \in H^1$,*

$$\|\Delta^{-1}(uv)w\|_{H^1} \leq K_0 (\|u\|_{H^1} \|v\|_{H^1} \|w\|_{L_2} + \|u\|_{H^1} \|v\|_{L_2} \|w\|_{H^1}) \tag{3.42}$$

and for $u, v, w \in H^2$,

$$\|\Delta^{-1}(uv)w\|_{H^2} \leq K_0 \sum_{(k,l,m)} \|u\|_{H^k} \|v\|_{H^l} \|w\|_{H^m} \tag{3.43}$$

with the sum being over all permutations (k,l,m) of (0,1,2).

Theorem 3.7.3. *The numerical solution ψ_n given by the Strang Splitting scheme (3.39) for the cubic nonlinear Schrödinger equation with step size $\tau > 0$ has a first-order error bound in H^2 and a second-order error bound in L_2,*

$$\begin{aligned} &\|\psi_n - \psi(t_n)\|_{H^2} \leq C(m_4, T)\tau \\ &\|\psi_n - \psi(t_n)\|_{L_2} \leq C(m_4, T)\tau^2 \end{aligned} \qquad for\ t_n = n\tau \leq T$$

.

Proposition 1. *(Stability) If $\psi, \phi \in H^2$ with*

$$\|\psi\|_{H^2} \leq M_2 \quad \|\phi\|_{H^2} \leq M_2$$

then

$$\|\Phi_\tau(\psi) - \Phi_\tau(\phi)\|_{L_2} \leq e^{c_0\tau}\|\psi - \phi\|_{L_2},$$

$$\|\Phi_\tau(\psi) - \Phi_\tau(\phi)\|_{H^1} \leq e^{c_1\tau}\|\psi - \phi\|_{H^1},$$

$$\|\Phi_\tau(\psi) - \Phi_\tau(\phi)\|_{H^1} \leq e^{c_2\tau}\|\psi - \phi\|_{H^2},$$

where c_0, c_1, c_2 only depend on M_2.

Proposition 2. *(Local error in L_2) If $\psi_0 \in H^4$ with $\|\psi_0\|_{H^4} \leq M_4$ then the error after one step of the method (3.39) is bounded in the L_2 norm by*

$$\|\psi_1 - \psi(\tau)\|_{L_2} \leq C_4\tau^2,$$

where C_4 only depends on M_4

CHAPTER 4

NUMERICAL SIMULATIONS

In this section we first look at the graphs of the solutions to the GPE at various times and for various potentials. Then we analyze the error bounds that were discussed at the end of the chapter 3 from [14]. First we will consider the case where $V = 0$ and vary the step size $dt = k$ and then vary the mesh factor $h = \frac{1}{M}$. All simulations will be run in two dimensions.

4.1 Example 1: ψ_0 as Gaussian

The first example will be a 2d defocusing case ($\kappa > 0$) with the initial condition

$$\psi(x, 0) = \frac{1}{\sqrt{\varepsilon\pi}} e^{-(x^2+y^2)/2\varepsilon} \tag{4.1}$$

This initial data will be used for all simulations.

4.1.1 $V = 0$

For a matter of perspective, we will run simulations for the case of $V = 0$ in the cubic nonlinear Schrödinger equation, i.e.

$$i\varepsilon \frac{\partial \psi(\mathbf{x}, t)}{\partial t} = -\frac{\varepsilon^2 \nabla^2}{2} \psi(\mathbf{x}, t) + \kappa |\psi(\mathbf{x}, t)|^2 \psi(\mathbf{x}, t) \tag{4.2}$$

with $\Delta t = .01$ the time step, $h = \frac{1}{32}$ corresponding with a mesh size that has $M = 512$ intervals, and $x \in [-8, 8]$.

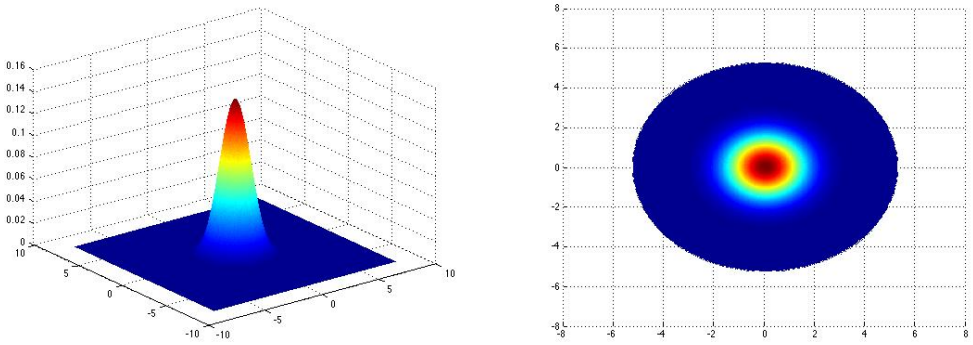

(a) 3d View (b) Top View

Figure 4.1: Solution to cubic NLS with $V = 0$, $t = 1$, $\Delta t = .01$, $h = 1/32$ and $(x, y) \in [-8, 8]^2$

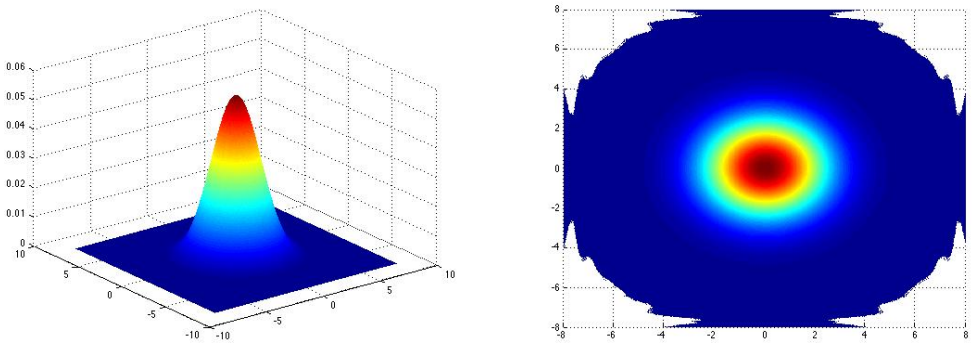

(a) 3d View (b) Top View

Figure 4.2: Solution to cubic NLS with $V = 0$, $t = 2$, $\Delta t = .01$, $h = 1/32$ and $(x, y) \in [-8, 8]^2$

The previous two figures 4.1 and 4.2 are the graphical representations of the solutions to this initial value problem at $t = 1$ and $t = 2$, respectively. The following figure represents a similar simulation where $x \in [-16, 16]$ with $\Delta t = .01$ and $M = 512$ corresponding to a mesh size of $h = \frac{1}{32}$.

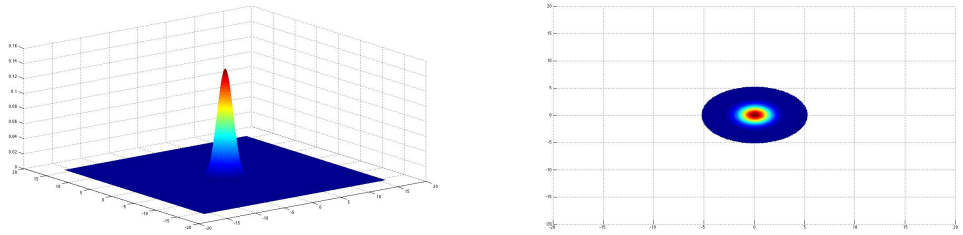

(a) 3d View (b) Top View

Figure 4.3: Solution to cubic NLS with $V = 0$, $t = 1$, $\Delta t = .01$, $h = 1/32$ and $(x, y) \in [-16, 16]^2$

4.1.2 $V = \frac{(x^2+y^2)}{2}$

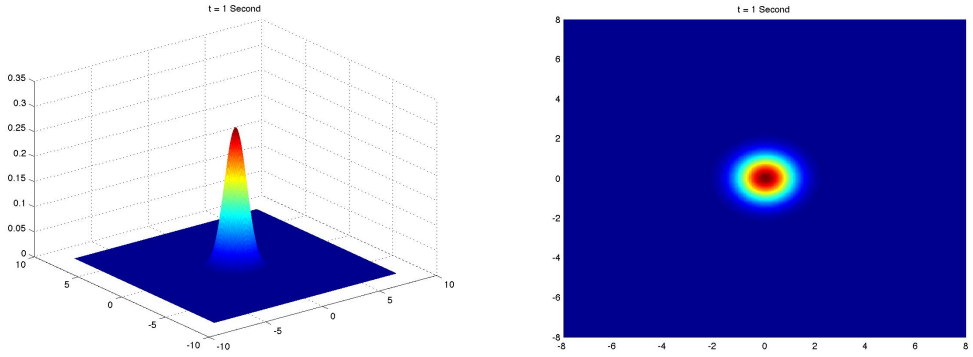

(a) 3d View (b) Top View

Figure 4.4: Solution to cubic NLS with $V = \frac{x^2+y^2}{2}$, $t = 1s$, $\Delta t = .001$, $h = 1/16$ and $(x, y) \in [-8, 8]^2$

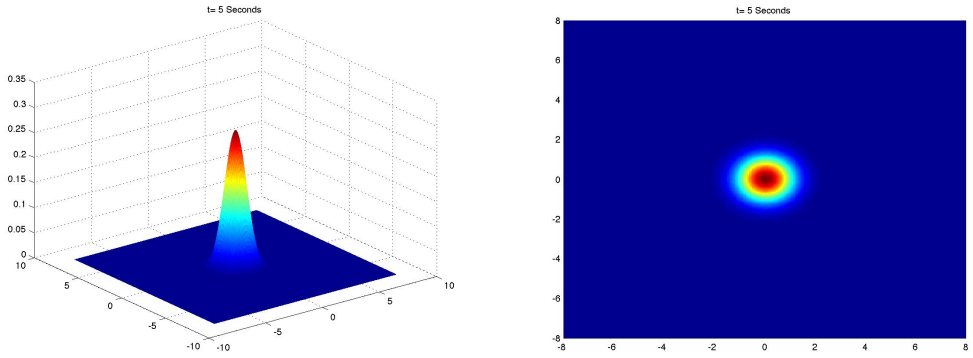

(a) 3d View (b) Top View

Figure 4.5: Solution to cubic NLS with $V = \frac{x^2+y^2}{2}$, $t = 5s$, $\Delta t = .001$, $h = 1/16$ and $(x, y) \in [-8, 8]^2$

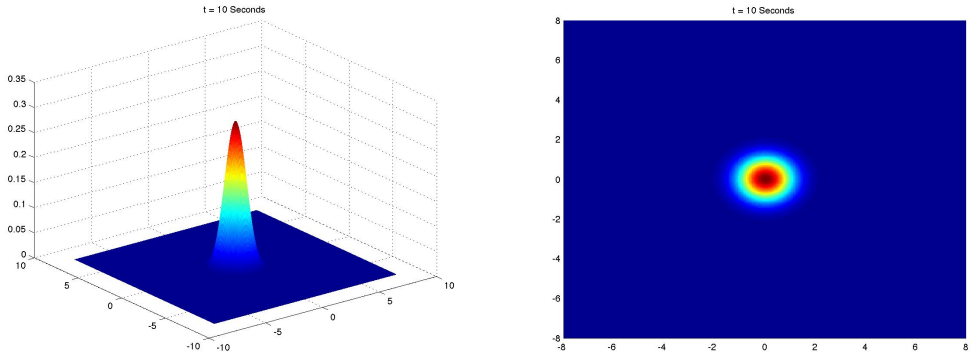

(a) 3d View (b) Top View

Figure 4.6: Solution to cubic NLS with $V = \frac{x^2+y^2}{2}$, $t = 10$, $\Delta t = .001$, $h = 1/16$ and $(x, y) \in [-8, 8]^2$

4.1.3 $V = \frac{(x^2+4y^2)}{2}$

A slight variation on the isotropic harmonic potential is the anisotropic potential:

$$V = \frac{(x^2 + 4y^2)}{2} \tag{4.3}$$

The following represent the solutions to the anisotropic GPE at time $t = 1$ then $t = 2$.

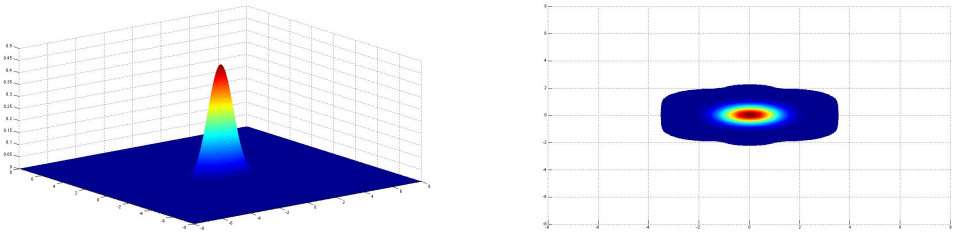

(a) 3d View (b) Top View

Figure 4.7: Solution to cubic NLS with $V = \frac{x^2+4y^2}{2}$, $t = 1$, $\Delta t = .01$, $h = 1/32$ and $(x, y) \in [-8, 8]^2$

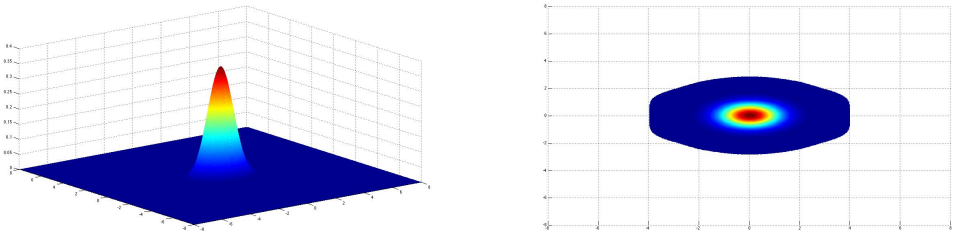

(a) 3d View (b) Top View

Figure 4.8: Solution to cubic NLS with $V = \frac{x^2+4y^2}{2}$, $t = 2$, $\Delta t = .01$, $h = 1/32$ and $(x, y) \in [-8, 8]^2$

4.1.4 $V = \frac{(x^2-y^2)}{2}$

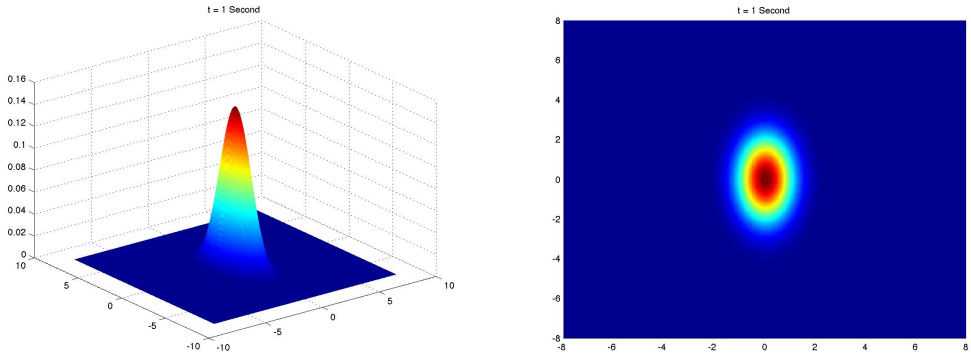

(a) 3d View (b) Top View

Figure 4.9: Solution to cubic NLS with $V = \frac{x^2-y^2}{2}$, $t = 1s$, $\Delta t = .001$, $h = 1/16$ and $(x, y) \in [-8, 8]^2$

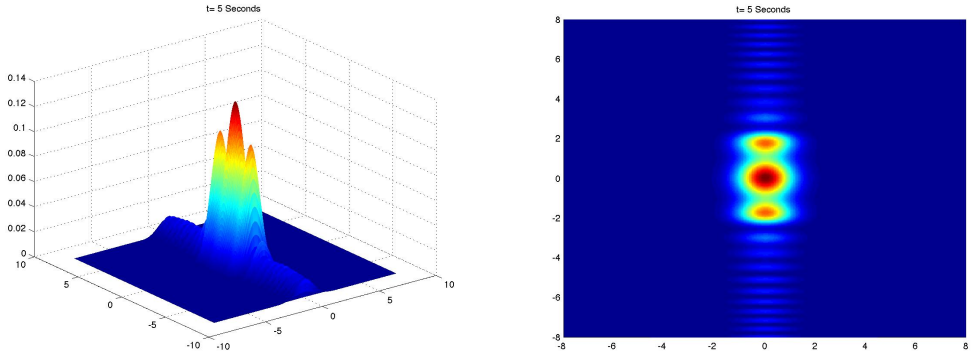

(a) 3d View (b) Top View

Figure 4.10: Solution to cubic NLS with $V = \frac{x^2-y^2}{2}$, $t = 5s$, $\Delta t = .01$, $h = 1/16$ and $(x, y) \in [-8, 8]^2$

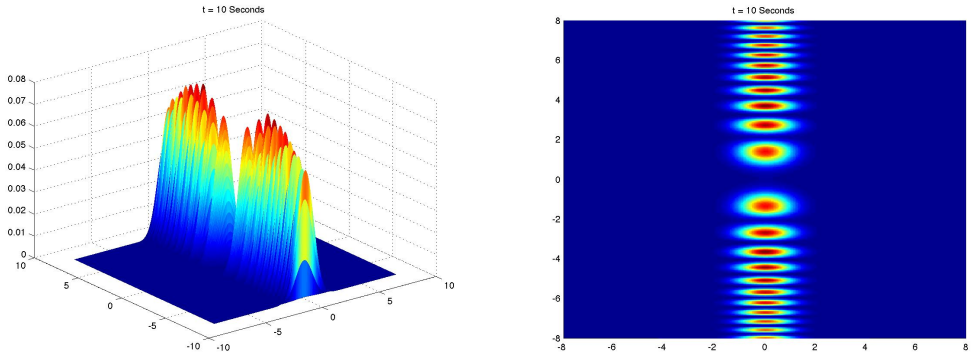

(a) 3d View (b) Top View

Figure 4.11: Solution to cubic NLS with $V = \frac{x^2-y^2}{2}$, $t = 10$, $\Delta t = .001$, $h = 1/16$ and $(x, y) \in [-8, 8]^2$

4.1.5 $V = \frac{-(x^2+y^2)}{2}$

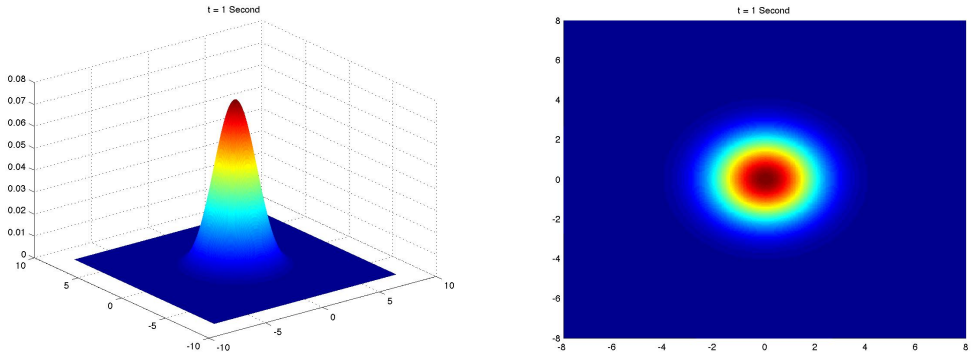

(a) 3d View (b) Top View

Figure 4.12: Solution to cubic NLS with $V = \frac{-(x^2+y^2)}{2}$, $t = 1s$, $\Delta t = .001$, $h = 1/16$ and $(x, y) \in [-8, 8]^2$

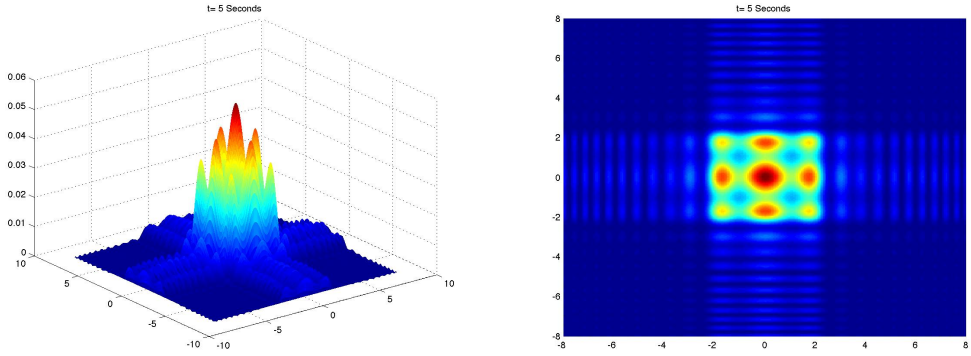

(a) 3d View (b) Top View

Figure 4.13: Solution to cubic NLS with $V = \frac{-(x^2+y^2)}{2}$, $t = 5s$, $\Delta t = .01$, $h = 1/16$ and $(x, y) \in [-8, 8]^2$

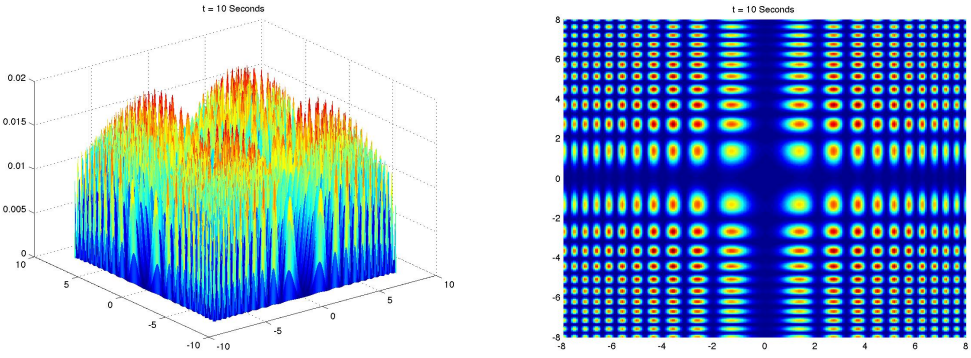

(a) 3d View (b) Top View

Figure 4.14: Solution to cubic NLS with $V = \frac{-(x^2+y^2)}{2}$, $t = 10$, $\Delta t = .001$, $h = 1/16$ and $(x, y) \in [-8, 8]^2$

4.1.6 $V = \frac{-(x^2+400y^2)}{2}$

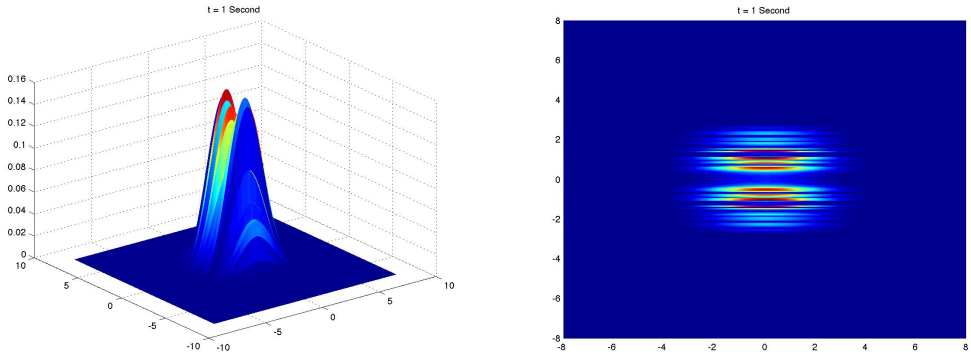

(a) 3d View (b) Top View

Figure 4.15: Solution to cubic NLS with $V = \frac{-(x^2+400y^2)}{2}$, $t = 1s$, $\Delta t = .001$, $h = 1/16$ and $(x, y) \in [-8, 8]^2$

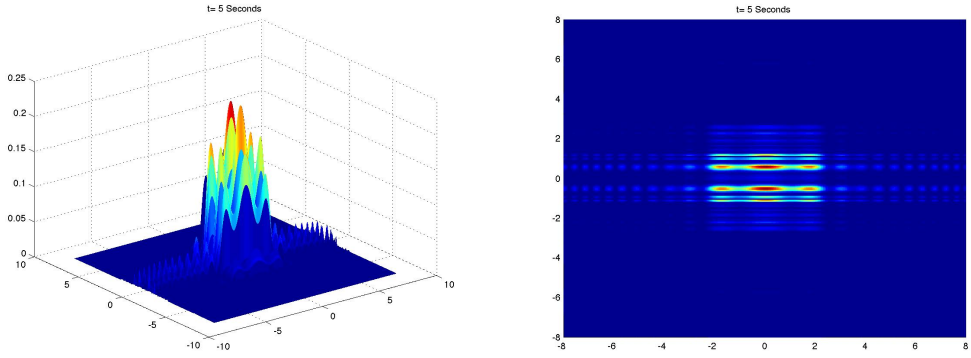

(a) 3d View (b) Top View

Figure 4.16: Solution to cubic NLS with $V = \frac{-(x^2+400y^2)}{2}$, $t = 5s$, $\Delta t = .01$, $h = 1/16$ and $(x, y) \in [-8, 8]^2$

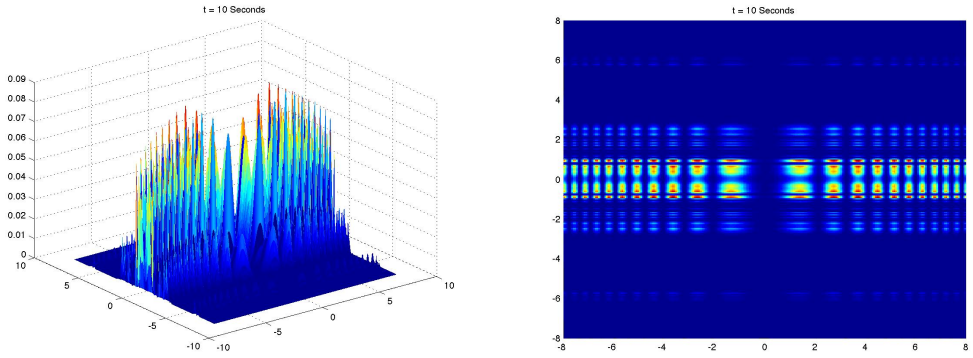

(a) 3d View (b) Top View

Figure 4.17: Solution to cubic NLS with $V = \frac{-(x^2+400y^2)}{2}$, $t = 10$, $\Delta t = .001$, $h = 1/16$ and $(x, y) \in [-8, 8]^2$

4.2 Focusing case: $\kappa < 0$

Recall equation (3.1)

$$iu_t = -\frac{u_{xx}(x,t)}{2} + \frac{x^2}{2}u(x,t) + \kappa_1|u(x,t)|^2u(x,t), \ a < x < b,$$

It is also relevant to analyze a situation where $\kappa < 0$ (the focusing case). Here we wish to only look at the visual realization of the solution and not analyze the error. We will continue to use the same initial condition as in previous sections (4.1).

The physics of the problem dictates that a positive harmonic potential is an attractive presence and will "trap" the BEC similarly to how the $\kappa < 0$ condition focuses the BEC. What we'd like to find out is if it's possible to flip the potential (i.e. a negative $V(x)$ which would attempt to disperse the solution to the wave equation) and offset the impact of the focusing κ.

The following simulations vary the magnitude of the negative coefficient of $\frac{x^2+y^2}{2}$ and graphs the impact of the time of blow-up.

4.2.1 $\kappa = -1.9718$

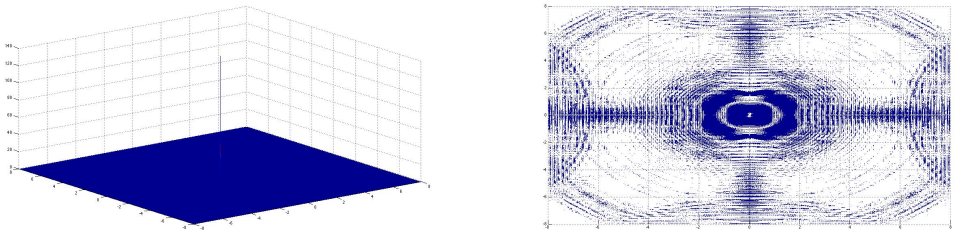

(a) 3d View

(b) Top View

Figure 4.18: Solution to cubic NLS with $V = 0$, $t = 1$, $\Delta t = .01$, $h = 1/32$, $\kappa = -1.9718$, and $(x, y) \in [-8, 8]^2$

This graphic represents the square of the wave function (position density) for the case $\kappa = -1.9718$ at time $t = 1$. Clearly, the singularity effect has happened in this case where $V = 0$.

For the remaining simulations, we vary the magnitude of the coefficient of the inverted harmonic potential to see the effects on the blow up time for the solution of the cubic NLS.

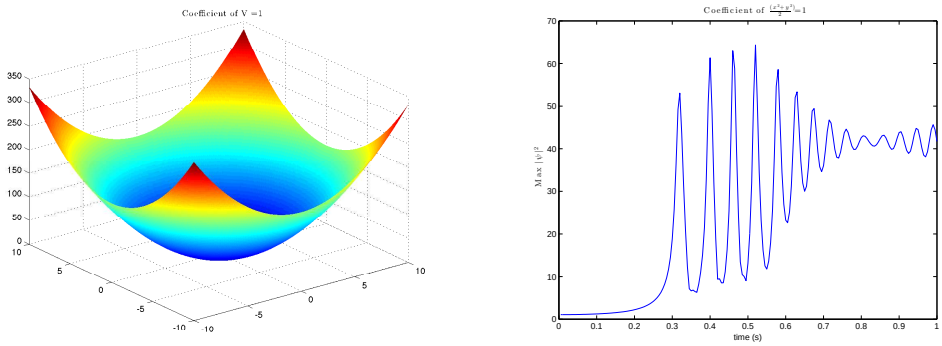

(a) $V = \frac{(x^2+y^2)}{2\varepsilon}$ (b) Maximum Value of $|\psi|^2$ vs time

Figure 4.19: Focusing case for $V = \frac{(x^2+y^2)}{2\varepsilon}, \varepsilon = 0.3, t = 1$s

Here we have a positive coefficient for the harmonic potential. A blow up time of approximately 0.3 seconds is observed. Wild oscillations follow the blow up time.

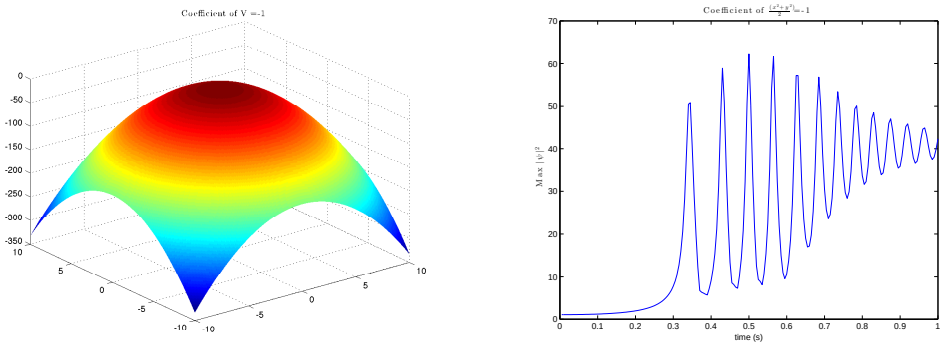

(a) $V = \frac{-(x^2+y^2)}{2\varepsilon}$ (b) Maximum Value of $|\psi|^2$ vs time

Figure 4.20: Focusing case for $V = \frac{-(x^2+y^2)}{2\varepsilon}, \varepsilon = 0.3, t = 1$s

Now we see from the left figure that the harmonic potential has been flipped upside down with a negative coefficient, $V = \frac{-(x^2+y^2)}{2\varepsilon}$, and upon close observation, the blow up time has been delayed slightly between 0.3s and 0.4s. With a coefficient of -1, the slope of the quadratic is identical to the initial potential, $\left(V = \frac{(x^2+y^2)}{2\varepsilon}\right)$, except negative.

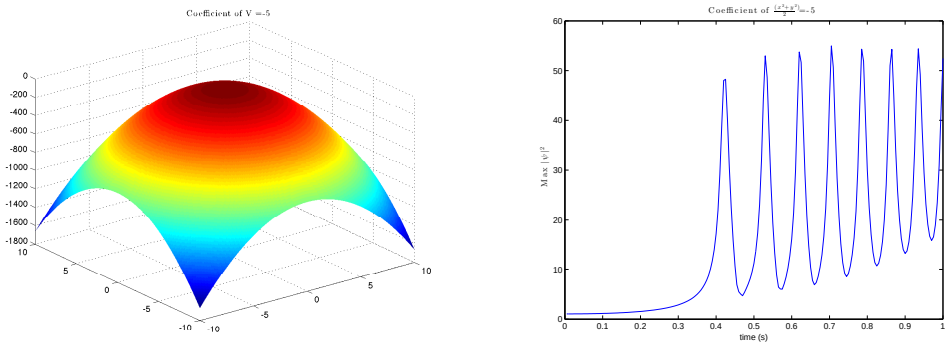

(a) $V = \frac{-5(x^2+y^2)}{2\varepsilon}$ (b) Maximum Value of $|\psi|^2$ vs time

Figure 4.21: Focusing case for $V = \frac{-5(x^2+y^2)}{2\varepsilon}, \varepsilon = 0.3, t = 1$s

Now, we increase the magnitude of the slope of the quadratic potential with the intent of increasing the effect. Note the blow up time has been increased to after 0.4 seconds.

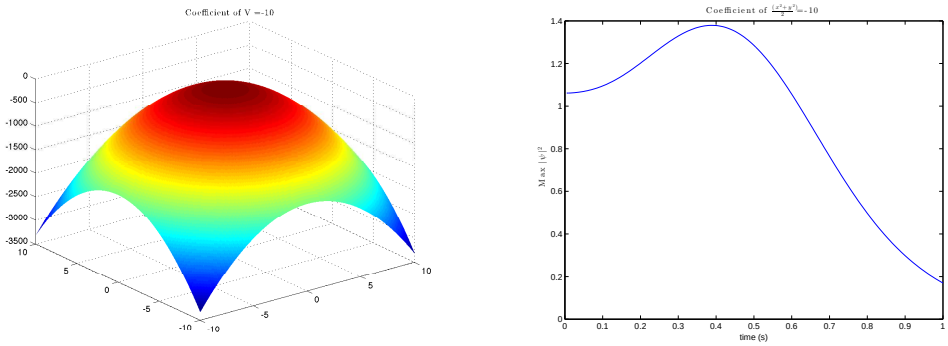

(a) $V = \frac{-10(x^2+y^2)}{2\varepsilon}$ (b) Maximum Value of $|\psi|^2$ vs time

Figure 4.22: Focusing case for $V = \frac{-10(x^2+y^2)}{2\varepsilon}, \varepsilon = 0.3, t = 1\text{s}$

Here, with the coefficient of the harmonic potential being -10, it appears as though the blow up time is completely gone. However it is important to note the time frame of the second graphic, $t \in [0, 1]$. Later, we will stretch that window to see if we can find the spike in magnitude of the position density.

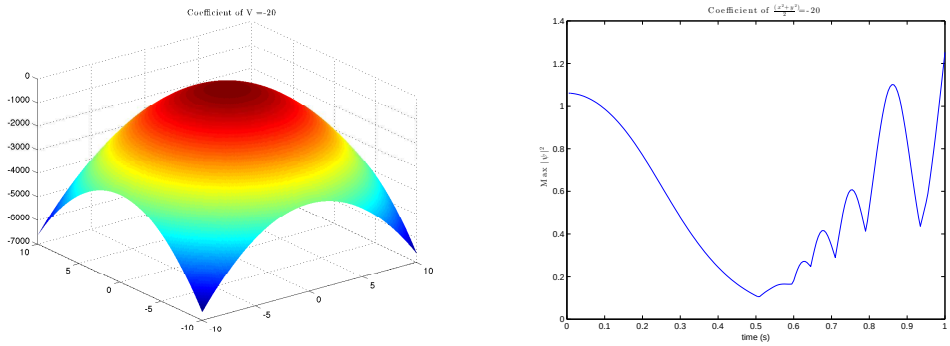

(a) $V = \frac{-20(x^2+y^2)}{2\varepsilon}$ (b) Maximum Value of $|\psi|^2$ vs time

Figure 4.23: Focusing case for $V = \frac{-20(x^2+y^2)}{2\varepsilon}, \varepsilon = 0.3, t = 1\text{s}$

As before, it appears as though the blow up of the position density has been eliminated but on the [0,1] interval only.

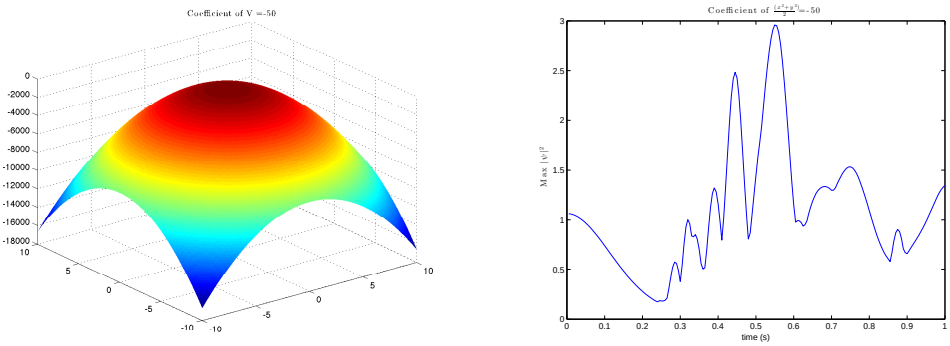

(a) $V = \frac{-50(x^2+y^2)}{2\varepsilon}$ (b) Maximum Value of $|\psi|^2$ vs time

Figure 4.24: Focusing case for $V = \frac{-50(x^2+y^2)}{2\varepsilon}, \varepsilon = 0.3, t = 1\text{s}$

Again, no blow up but note the increase in the high end of the position density. Also there are wild oscillations in this [0,1] time window.

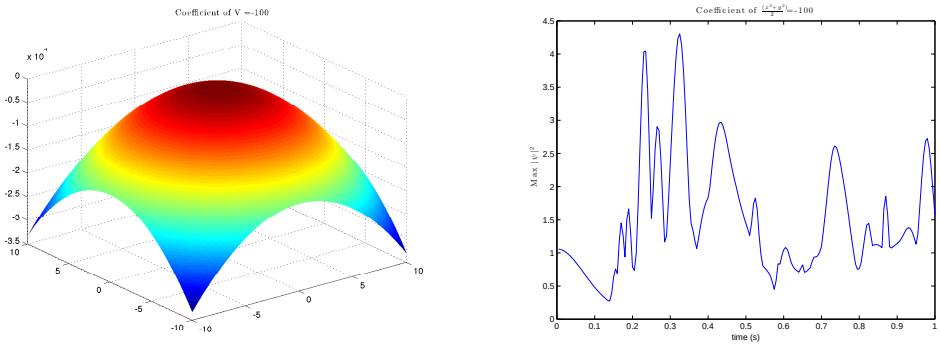

(a) $V = \frac{-100(x^2+y^2)}{2\varepsilon}$ (b) Maximum Value of $|\psi|^2$ vs time

Figure 4.25: Focusing case for $V = \frac{-100(x^2+y^2)}{2\varepsilon}, \varepsilon = 0.3, t = 1$s

The final simulation on the [0,1] time interval. As compared to $V(x) = \frac{-50(x^2+y^2)}{2\varepsilon}$, this potential causes the solution position density to vary wildly within the 0 to 4.5 range. Next we observe the time interval $t \in [0, 5]$ to see the impact of the greater slope on the quadratic potential.

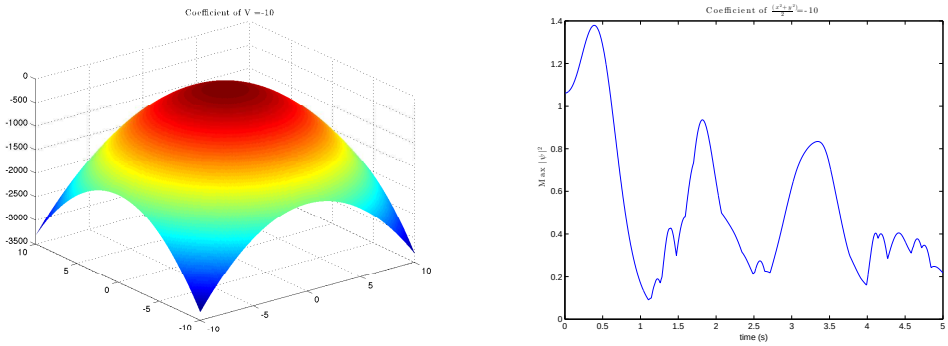

(a) $V = \frac{-10(x^2+y^2)}{2\varepsilon}$ (b) Maximum Value of $|\psi|^2$ vs time

Figure 4.26: Focusing case for $V = \frac{-10(x^2+y^2)}{2\varepsilon}, \varepsilon = 0.3, t = 5$s

For this scenario we return to the potential $V = \frac{-10(x^2+y^2)}{2\varepsilon}$ and extend the time window to $t \in [0, 5]$. Note for this case, there still does not appear to be a spike in the position density. We will return to this again on a longer interval later.

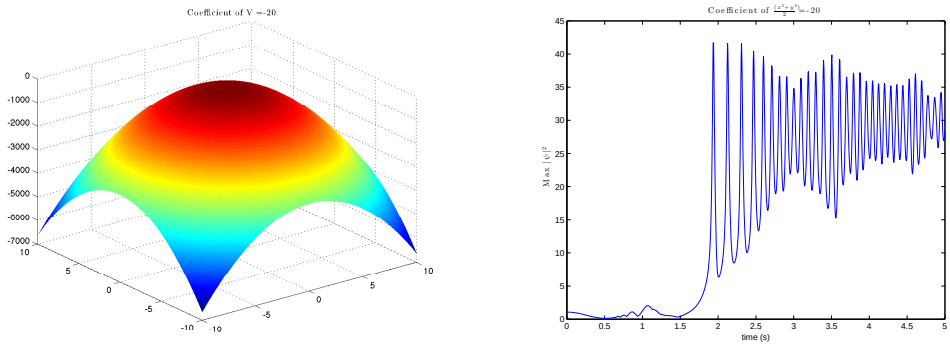

(a) $V = \frac{-20(x^2+y^2)}{2\varepsilon}$ (b) Maximum Value of $|\psi|^2$ vs time

Figure 4.27: Focusing case for $V = \frac{-20(x^2+y^2)}{2\varepsilon}, \varepsilon = 0.3, t = 5$s

Finally when we expand the time window for $V = \frac{-20(x^2+y^2)}{2\varepsilon}$ we find the blow up at just prior to 2 seconds. Wild oscillations in the max of the position density are found following this time.

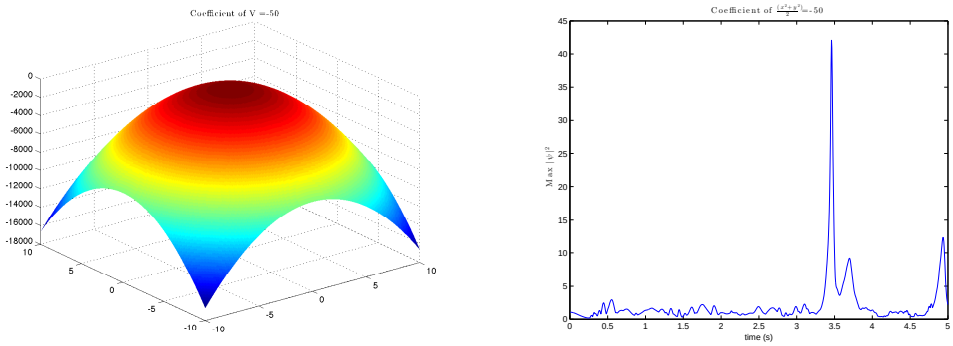

(a) $V = \frac{-50(x^2+y^2)}{2\varepsilon}$ (b) Maximum Value of $|\psi|^2$ vs time

Figure 4.28: Focusing case for $V = \frac{-50(x^2+y^2)}{2\varepsilon}, \varepsilon = 0.3, t = 5$s

Here we see the blow up occurence pushed to approximately 3.5 seconds in the $t \in [0, 5]$ window. In the case of $V = \frac{-100(x^2+y^2)}{2\varepsilon}$, on the next page, the blow up time is roughly 2.5 seconds.

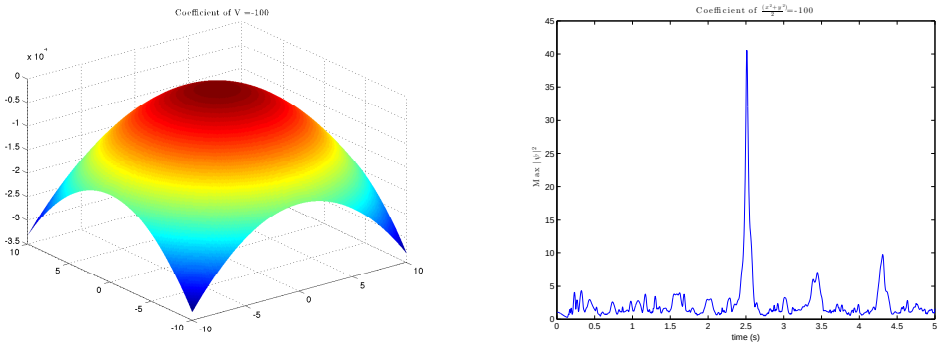

(a) $V = \frac{-100(x^2+y^2)}{2\varepsilon}$ (b) Maximum Value of $|\psi|^2$ vs time

Figure 4.29: Focusing case for $V = \frac{-100(x^2+y^2)}{2\varepsilon}, \varepsilon = 0.3, t = 5\text{s}$

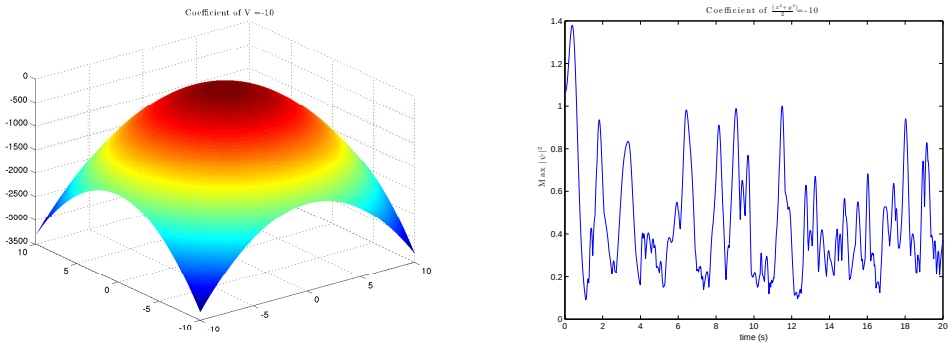

(a) $V = \frac{-10(x^2+y^2)}{2\varepsilon}$ (b) Maximum Value of $|\psi|^2$ vs time

Figure 4.30: Focusing case for $V = \frac{-10(x^2+y^2)}{2\varepsilon}, \varepsilon = 0.3, t = 20$s

Finally we attempt to see the blow up for the case of $V = \frac{-10(x^2+y^2)}{2\varepsilon}$ by expanding the time frame to [0,20], but do not see any.

4.3 Error Testing

In this section we will analyze the errors in space and time and compare to Lubich [14].

4.3.1 Spatialization Errors

Here we analyze errors in the discretization of the space variable. A very small time step is chosen ($\Delta t = .0001$) for the Gaussian initial condition from earlier (4.1) and the spatial discretization is taken as a progressively finer and finer mesh in two dimensions. The discretization as well as the boundaries for the x and y directions will be taken to be equal.

Potential	$h = \frac{1}{4}$	$h = \frac{1}{8}$	$h = \frac{1}{16}$	$h = \frac{1}{32}$
0	2.5353e-05	1.2107e-11	3.4148e-12	1.3345e-11
$\frac{(x^2+y^2)}{2\varepsilon}$	1.8215e-05	4.0089e-10	1.7532e-10	8.5637e-11
$10\frac{(x^2+y^2)}{2\varepsilon}$	1.7633e-01	2.3737e-03	2.8753e-09	6.9805e-12
$-1\frac{(x^2+y^2)}{2\varepsilon}$	8.7515e-04	9.0129e-06	3.3705e-06	1.5221e-06
$\frac{(10x^2+y^2)}{2\varepsilon}$	1.7456e-01	1.3289e-03	7.5564e-10	7.9029e-11
$\frac{(x^2+10y^2)}{2\varepsilon}$	1.7456e-01	1.3289e-03	7.5563e-10	7.9029e-11
$\frac{(x^2-10y^2)}{2\varepsilon}$	2.7557e+00	4.8414e+00	3.5978e+00	5.0977e-02

Table 4.1: Spatial discretization error analysis $\|\psi - \psi_{h,k}\|_{l^2}$ at $t = 1$ on $[a, b] = [-8, 8]$ with $\Delta t = .00005$

4.3.2 Temporal Errors

In this section we analyze the error in the time stepping. We choose a particular spatial discretization ($M = 512, h = \frac{1}{32}$) and then vary the size of the time step. The following data represents this test for both $V = 0$ and for the harmonic potential $V = \frac{(x^2+y^2)}{2}$

Potential	$\Delta t = 0.01$	$\Delta t = 0.005$	$\Delta t = 0.0025$	$\Delta t = 0.00125$	$\Delta t = 0.000625$
0	2.5615e-03	6.3592e-04	1.5871e-04	3.9662e-05	9.9139e-06
$\frac{(x^2+y^2)}{2\varepsilon}$	1.3647e-02	3.4068e-03	8.5140e-04	2.1283e-04	5.3203e-05
$10\frac{(x^2+y^2)}{2\varepsilon}$	5.4547e-01	1.2043e-01	2.9065e-02	7.2394e-03	1.8082e-03
$-1\frac{(x^2+y^2)}{2\varepsilon}$	4.9640e-02	1.2426e-02	3.1075e-03	7.7695e-04	1.9425e-04
$\frac{(10x^2+y^2)}{2\varepsilon}$	2.7675e-01	6.7647e-02	1.6747e-02	4.1805e-03	1.0447e-03
$\frac{(x^2+10y^2)}{2\varepsilon}$	2.7675e-01	6.7647e-02	1.6747e-02	4.1805e-03	1.0447e-03
$\frac{(x^2-10y^2)}{2\varepsilon}$	1.3843e+01	4.1819e+00	1.1328e+00	3.1327e-01	5.5413e-02

Table 4.2: Temporal discretization error analysis $\|\psi - \psi_{h,k}\|_{l^2}$ at $t = 1$ on $[a, b] = [-8, 8]$ with $h = \frac{1}{64}$

CHAPTER 5

CONCLUSION

In the study of Bose-Einstein Condensation, the Gross-Pitaevskii yields solutions which are not analytic and thus must be solved numerically. Many methods have been proposed in order to solve this nonlinear Schrödinger equation, but in particular the Strang Splitting method has been shown to be very accurate and not very taxing on the computer systems that utilize it. Bao, et al [4] showed that this spectral splitting method is found to be more accurate and faster than both the Crank-Nicolson Finite Difference method and the Crank-Nicolson spectral method when solving the linear Schrödinger equation numerically.

Lubich [14] proved error bounds in H^2 and L_2 for the Strang Splitting method for cubic nonlinear Schrödinger equations with initial data $\psi_0 \in H^4$. In the simulations run in this thesis, the choice of initial data is

$$\psi_0 = \frac{1}{\sqrt{\pi}} e^{\frac{-(x^2+y^2)}{2}}.$$

Clearly $\psi_0 \in H^4$ and thus we verified Lubich's error bounds with different potentials $V(x, y)$ in Tables (4.1), and (4.2)

Next the graphs of solutions for $V(x, y) = 0$ were shown to agree with the physical theory. In the presence of no trapping potential (attractive) a cubic nonlinearity with a positive interaction coefficient ($\kappa > 0$, defocusing) will cause the wave to dissipate as was seen in fig. (4.1) and fig (4.2). When an isotropic harmonic potential ($\frac{(x^2+y^2)}{2\varepsilon}$) was turned on, we find the condensate will oscillate based on the attractive characteristics of the quadratic potential with the repulsive characteristics of the cubic nonlinearity. This is verified, although not easy to see, by figs (4.4), (4.5), (4.6). The center of the solution does slightly widen, then shrink again and the center darkest part does change size, only to oscillate.

Figures (4.7) through (4.17) represent varying forms of the harmonic potential

(isotropic, anisotropic, negative coefficient). The outcome of the simulation is a solution which again agree with the physics of the BEC. Recalling the scaling parameters (2.15) introduced in order to make the GPE dimensionless, we can see that the differences in frequencies in the x and y domains would cause the oscillations of the condensates to be different in the corresponding x and y directions (cf. Figures (4.7) and (4.8)). In the cases where negative frequencies (ratios, again see (2.15)) are used in either the x-direction, the y-direction (or both) we would expect to see a dissipative pattern over time (in addition to the dissipative quality of the cubic nonlinearity in the defocusing case) and we do. For $\gamma_y < 0$ with $\gamma_x > 0$ we see dissipation in only the y-direction (cf. Figures (4.9) - (4.11)). When the coefficient of the entire potential is negative, (i.e. repulsive in both the x- and y-direction) the entire wave function dissipates at rates that we would expect [10], [11].

Finally the case of the focusing Bose Einstein Condensate was analyzed. The focusing nonlinearity causes an attractive effect on the condensate that can cause it to "blow up" in finite time (4.18). The simulations run were intended to counteract this effect through a harmonic potential that was now switched to negative frequency i.e. repulsive. The graphs of solutions show that blow up time would be impacted by the magnitude of the coefficient of the potential in addition to the sign change. Simply changing the sign alone and keeping the magnitude of the coefficient as 1 in the first simulation figs (4.19) and (4.20). Potentials with a greater magnitude (slope) tended to push the blow up time even further (cf. (4.30), (4.27), and (4.28))

Appendix A

GPE SOLVING CODE

In this section the MATLAB code is presented that was used to solve the GPE. Initially, this code was used, but special thanks is given to Xavier Antoine and Romain Duboscq for GPELab [1], an open source MATLAB package that greatly sped up the simulation process.

```
function solution = gpesolve(Lx,Nx,tf,dt, eps, K, Vi)


% set up gridt_total=2; % total time in seconds
 % time step
Nt= tf/dt;% number of time slices
Ny=Nx;
Ly=Lx;
% initialise variables
x = (-Lx:2*Lx/Nx:Lx-2*Lx/Nx)'; % x coordinate
kx = pi*[0:Nx/2-1 0 -Nx/2+1:-1]'/(Lx); % wave vector
y = (-Ly:2*Ly/Ny:Ly-2*Ly/Ny)'; % y coordinate
ky = pi*[0:Ny/2-1 0 -Ny/2+1:-1]'/(Ly); % wave vector
[xx,yy]=meshgrid(x,y);
[k2xm,k2ym]=meshgrid(kx.^2,ky.^2);
% initial conditions
u =(1/sqrt(pi*eps))*exp((-.5/eps)*(xx.^2+yy.^2));
%u = ((2^(1/4))/sqrt(pi*eps))*exp((-.5/eps)*(xx.^2+2*yy.^2)).*exp((1/eps)*1i*
%v=fft2(u(:,:,1));
if Vi == 1
    V = (xx.^2 + 4*yy.^2)/2;
```

```
elseif Vi==2
        V = (xx.^2 + yy.^2)/2;
    else
    V=zeros(Nx);
end
% solve pde and plot results
for n =2:Nt+1
    pot1=V + K*(abs(u)).^2;
    unb=exp(-1i*(dt/(2*eps))*pot1).*u;
    vnb=fft2(unb);
    vna=exp(-.5*1i*eps*dt*(k2xm + k2ym)).*vnb;
    una=ifft2(vna);
    pot2=V + K*(abs(una)).^2;
    u=exp(-1i*(dt/(2*eps))*pot2).*una;
    maximum(n-1)= max(max(abs(u).^2));
    if (mod(n-1,10)==0) %%Plot solutions for each time interval
        figure(2); clf; surf(xx,yy,abs(u).^2,'EdgeColor','none'); title(nun
        drawnow;
    end

end
solution = u;
```

Appendix B

TESTING THE GPE SOLVER

This code calls the previous gpesolve.m function and stores the output as N matrices where $N = \frac{t_f}{dt}$. Files were created and saved with names based on the specification of the problem. For example "V0M32dt000188" represents a potential $V(x) = 0$, a spatial mesh size of 32, a time step of 0.0001 seconds and the interval is $(x, y) \in [-8, 8]^2$

```
%%%%%%%%%% Spatialization Error Tests V=0 t=1,dt=.0001 %%%%%%%%%%
V0M32dt000188 = gpesolve(8,32,1,.0001,1,1,0);
save V0M32dt000188 V0M32dt000188;

V0M64dt000188 = gpesolve(8,64,1,.0001,1,1,0);
save V0M64dt000188 V0M64dt000188;

V0M128dt000188 = gpesolve(8,128,1,.0001,1,1,0);
save V0M128dt000188 V0M128dt000188;

V0M256dt000188 = gpesolve(8,256,1,.0001,1,1,0);
save V0M256dt000188 V0M256dt000188;

V0M512dt000188 = gpesolve(8,512,1,.0001,1,1,0);
save V0M512dt000188 V0M512dt000188;

V0M2048dt0001EXACT88 = gpesolve(8,2048,1,.0001,1,1,0);
```

```
save V0M2048dt0001EXACT88 V0M2048dt0001EXACT88;

%%%%%%%%%%%%%%%%%%Time Tests for V=0, M=512 %%%%%%%%%%%%%%%%%%%%%%%%%%%%%%%%

V0M512dt0188 = gpesolve(8,512,1,.01,1,1,0);
save V0M512dt0188 V0M512dt0188;

V0M512dt00588 = gpesolve(8,512,1,.005,1,1,0);
save V0M512dt00588 V0M512dt00588;

V0M512dt002588 = gpesolve(8,512,1,.0025,1,1,0);
save V0M512dt002588 V0M512dt002588;

V0M512dt0012588 = gpesolve(8,512,1,.00125,1,1,0);
save V0M512dt0012588 V0M512dt0012588;

V0M512dt00062588 = gpesolve(8,512,1,.000625,1,1,0);
save V0M512dt00062588 V0M512dt00062588;

V0M512dt000001EXACT88 = gpesolve(8,512,1,.000001,1,1,0);
save V0M512dt000001EXACT88 V0M512dt000001EXACT88;


%%%%%%%%%% Spatialization Error Tests V=1 t=1,dt=.0001 %%%%%%%%%%
V1M32dt000188 = gpesolve(8,32,1,.0001,1,1,1);
save V1M32dt000188 V1M32dt000188;
```

```
V1M64dt000188 = gpesolve(8,64,1,.0001,1,1,1);
save V1M64dt000188 V1M64dt000188;

V1M128dt000188 = gpesolve(8,128,1,.0001,1,1,1);
save V1M128dt000188 V1M128dt000188;

V1M256dt000188 = gpesolve(8,256,1,.0001,1,1,1);
save V1M256dt000188 V1M256dt000188;

V1M512dt000188 = gpesolve(8,512,1,.0001,1,1,1);
save V1M512dt000188 V1M512dt000188;

V1M2048dt0001EXACT88 = gpesolve(8,2048,1,.0001,1,1,1);
save V1M2048dt0001EXACT88 V1M2048dt0001EXACT88;

%%%%%%%%%%%%%%%%%%Time Tests for V=1, M=512 %%%%%%%%%%%%%%%%%%%%%%%%%%%%%%%%

V1M512dt0188 = gpesolve(8,512,1,.01,1,1,1);
save V1M512dt0188 V1M512dt0188;

V1M512dt00588 = gpesolve(8,512,1,.005,1,1,1);
save V1M512dt00588 V1M512dt00588;

V1M512dt002588 = gpesolve(8,512,1,.0025,1,1,1);
save V1M512dt002588 V1M512dt002588;
```

```
V1M512dt0012588 = gpesolve(8,512,1,.00125,1,1,1);
save V1M512dt0012588 V1M512dt0012588;

V1M512dt00062588 = gpesolve(8,512,1,.000625,1,1,1);
save V1M512dt00062588 V1M512dt00062588;

V1M512dt000001EXACT88 = gpesolve(8,512,1,.000001,1,1,1);
save V1M512dt000001EXACT88 V1M512dt000001EXACT88;

%%%%%%%%% Spatialization Error Tests V=1 t=1,dt=.0001 %%%%%%%%%
V2M32dt000188 = gpesolve(8,32,1,.0001,1,1,2);
save V2M32dt000188 V2M32dt000188;

V2M64dt000188 = gpesolve(8,64,1,.0001,1,1,2);
save V2M64dt000188 V2M64dt000188;

V2M128dt000188 = gpesolve(8,128,1,.0001,1,1,2);
save V2M128dt000188 V2M128dt000188;

V2M256dt000188 = gpesolve(8,256,1,.0001,1,1,2);
save V2M256dt000188 V2M256dt000188;

V2M512dt000188 = gpesolve(8,512,1,.0001,1,1,2);
save V2M512dt000188 V2M512dt000188;
```

```
V2M2048dt0001EXACT88 = gpesolve(8,2048,1,.0001,1,1,2);
save V2M2048dt0001EXACT88 V2M2048dt0001EXACT88;

%%%%%%%%%%%%%%%%%Time Tests for V=1, M=512 %%%%%%%%%%%%%%%%%%%%%%%%%%%%%%%%

V2M512dt0188 = gpesolve(8,512,1,.01,1,1,2);
save V2M512dt0188 V2M512dt0188;

V2M512dt00588 = gpesolve(8,512,1,.005,1,1,2);
save V2M512dt00588 V2M512dt00588;

V2M512dt002588 = gpesolve(8,512,1,.0025,1,1,2);
save V2M512dt002588 V2M512dt002588;

V2M512dt0012588 = gpesolve(8,512,1,.00125,1,1,2);
save V2M512dt0012588 V2M512dt0012588;

V2M512dt00062588 = gpesolve(8,512,1,.000625,1,1,2);
save V2M512dt00062588 V2M512dt00062588;

V2M512dt000001EXACT88 = gpesolve(8,512,1,.000001,1,1,2);
save V2M512dt000001EXACT88 V2M512dt000001EXACT88;

%%%%%%%%%% Spatialization Error Tests V=0 t=1,dt=.0001 %%%%%%%%%%
V0M32dt000116 = gpesolve(16,32,1,.0001,1,1,0);
save V0M32dt000116 V0M32dt000116;
```

```
V0M64dt000116 = gpesolve(16,64,1,.0001,1,1,0);
save V0M64dt000116 V0M64dt000116;

V0M128dt000116 = gpesolve(16,128,1,.0001,1,1,0);
save V0M128dt000116 V0M128dt000116;

V0M256dt000116 = gpesolve(16,256,1,.0001,1,1,0);
save V0M256dt000116 V0M256dt000116;

V0M512dt000116 = gpesolve(16,512,1,.0001,1,1,0);
save V0M512dt000116 V0M512dt000116;

V0M2048dt000001EXACT16 = gpesolve(16,2048,1,.0001,1,1,0);
save V0M2048dt000001EXACT16 V0M2048dt000001EXACT16;

%%%%%%%%%%%%%%%%%%Time Tests for V=0, M=512 %%%%%%%%%%%%%%%%%%%%%%%%%%%%%%%%

V0M512dt0116 = gpesolve(16,512,1,.01,1,1,0);
save V0M512dt0116 V0M512dt0116;

V0M512dt00516 = gpesolve(16,512,1,.005,1,1,0);
save V0M512dt00516 V0M512dt00516;

V0M512dt002516 = gpesolve(16,512,1,.0025,1,1,0);
save V0M512dt002516 V0M512dt002516;
```

```
V0M512dt0012516 = gpesolve(16,512,1,.00125,1,1,0);
save V0M512dt0012516 V0M512dt0012516;

V0M512dt00062516 = gpesolve(16,512,1,.000625,1,1,0);
save V0M512dt00062516 V0M512dt00062516;

V0M512dt000001EXACT16 = gpesolve(16,512,1,.000001,1,1,0);
save V0M512dt000001EXACT16 V0M512dt000001EXACT16;


%%%%%%%%%% Spatialization Error Tests V=1 t=1,dt=.0001 %%%%%%%%%%
V1M32dt000116 = gpesolve(8,32,1,.0001,1,1,1);
save V1M32dt000116 V1M32dt000116;

V1M64dt000116 = gpesolve(16,64,1,.0001,1,1,1);
save V1M64dt000116 V1M64dt000116;

V1M128dt000116 = gpesolve(16,128,1,.0001,1,1,1);
save V1M128dt000116 V1M128dt000116;

V1M256dt000116 = gpesolve(16,256,1,.0001,1,1,1);
save V1M256dt000116 V1M256dt000116;

V1M512dt000116 = gpesolve(16,512,1,.0001,1,1,1);
save V1M512dt000116 V1M512dt000116;
```

```
V1M2048dt000001EXACT16 = gpesolve(16,2048,1,.0001,1,1,1);
save V1M2048dt000001EXACT16 V1M2048dt000001EXACT16;

%%%%%%%%%%%%%%%%%%Time Tests for V=1, M=512 %%%%%%%%%%%%%%%%%%%%%%%%%%%%%%%%

V1M512dt0116 = gpesolve(16,512,1,.01,1,1,1);
save V1M512dt0116 V1M512dt0116;

V1M512dt00516 = gpesolve(16,512,1,.005,1,1,1);
save V1M512dt00516 V1M512dt00516;

V1M512dt002516 = gpesolve(16,512,1,.0025,1,1,1);
save V1M512dt002516 V1M512dt002516;

V1M512dt0012516 = gpesolve(16,512,1,.00125,1,1,1);
save V1M512dt0012516 V1M512dt0012516;

V1M512dt00062516 = gpesolve(16,512,1,.000625,1,1,1);
save V1M512dt00062516 V1M512dt00062516;

V1M512dt000001EXACT16 = gpesolve(16,512,1,.000001,1,1,1);
save V1M512dt000001EXACT16 V1M512dt000001EXACT16;
```

Appendix C

ERROR TESTING

Files in this section were named similarly as before, but these files store the value of the error between the "exact" solution (very fine mesh, small dt) and the approximate solution.

```
%%%%%%%%%% Spatialization Error Tests V=0 t=1,dt=.0001 %%%%%%%%%%
V0M32dt000188 = gpesolve(8,32,1,.0001,1,1,0);
save V0M32dt000188 V0M32dt000188;

V0M64dt000188 = gpesolve(8,64,1,.0001,1,1,0);
save V0M64dt000188 V0M64dt000188;

V0M128dt000188 = gpesolve(8,128,1,.0001,1,1,0);
save V0M128dt000188 V0M128dt000188;

V0M256dt000188 = gpesolve(8,256,1,.0001,1,1,0);
save V0M256dt000188 V0M256dt000188;

V0M512dt000188 = gpesolve(8,512,1,.0001,1,1,0);
save V0M512dt000188 V0M512dt000188;

V0M2048dt0001EXACT88 = gpesolve(8,2048,1,.0001,1,1,0);
save V0M2048dt0001EXACT88 V0M2048dt0001EXACT88;
```

```
%%%%%%%%%%%%%%%%%%Time Tests for V=0, M=512 %%%%%%%%%%%%%%%%%%%%%%%%%%%%%%%%

V0M512dt0188 = gpesolve(8,512,1,.01,1,1,0);
save V0M512dt0188 V0M512dt0188;

V0M512dt00588 = gpesolve(8,512,1,.005,1,1,0);
save V0M512dt00588 V0M512dt00588;

V0M512dt002588 = gpesolve(8,512,1,.0025,1,1,0);
save V0M512dt002588 V0M512dt002588;

V0M512dt0012588 = gpesolve(8,512,1,.00125,1,1,0);
save V0M512dt0012588 V0M512dt0012588;

V0M512dt00062588 = gpesolve(8,512,1,.000625,1,1,0);
save V0M512dt00062588 V0M512dt00062588;

V0M512dt000001EXACT88 = gpesolve(8,512,1,.000001,1,1,0);
save V0M512dt000001EXACT88 V0M512dt000001EXACT88;


%%%%%%%%%% Spatialization Error Tests V=1 t=1,dt=.0001 %%%%%%%%%%
V1M32dt000188 = gpesolve(8,32,1,.0001,1,1,1);
save V1M32dt000188 V1M32dt000188;

V1M64dt000188 = gpesolve(8,64,1,.0001,1,1,1);
```

```
save V1M64dt000188 V1M64dt000188;

V1M128dt000188 = gpesolve(8,128,1,.0001,1,1,1);
save V1M128dt000188 V1M128dt000188;

V1M256dt000188 = gpesolve(8,256,1,.0001,1,1,1);
save V1M256dt000188 V1M256dt000188;

V1M512dt000188 = gpesolve(8,512,1,.0001,1,1,1);
save V1M512dt000188 V1M512dt000188;

V1M2048dt0001EXACT88 = gpesolve(8,2048,1,.0001,1,1,1);
save V1M2048dt0001EXACT88 V1M2048dt0001EXACT88;

%%%%%%%%%%%%%%%%%%Time Tests for V=1, M=512 %%%%%%%%%%%%%%%%%%%%%%%%%%%%%%%%

V1M512dt0188 = gpesolve(8,512,1,.01,1,1,1);
save V1M512dt0188 V1M512dt0188;

V1M512dt00588 = gpesolve(8,512,1,.005,1,1,1);
save V1M512dt00588 V1M512dt00588;

V1M512dt002588 = gpesolve(8,512,1,.0025,1,1,1);
save V1M512dt002588 V1M512dt002588;

V1M512dt0012588 = gpesolve(8,512,1,.00125,1,1,1);
```

```
save V1M512dt0012588 V1M512dt0012588;

V1M512dt00062588 = gpesolve(8,512,1,.000625,1,1,1);
save V1M512dt00062588 V1M512dt00062588;

V1M512dt000001EXACT88 = gpesolve(8,512,1,.000001,1,1,1);
save V1M512dt000001EXACT88 V1M512dt000001EXACT88;

%%%%%%%%% Spatialization Error Tests V=1 t=1,dt=.0001 %%%%%%%%%
V2M32dt000188 = gpesolve(8,32,1,.0001,1,1,2);
save V2M32dt000188 V2M32dt000188;

V2M64dt000188 = gpesolve(8,64,1,.0001,1,1,2);
save V2M64dt000188 V2M64dt000188;

V2M128dt000188 = gpesolve(8,128,1,.0001,1,1,2);
save V2M128dt000188 V2M128dt000188;

V2M256dt000188 = gpesolve(8,256,1,.0001,1,1,2);
save V2M256dt000188 V2M256dt000188;

V2M512dt000188 = gpesolve(8,512,1,.0001,1,1,2);
save V2M512dt000188 V2M512dt000188;

V2M2048dt0001EXACT88 = gpesolve(8,2048,1,.0001,1,1,2);
save V2M2048dt0001EXACT88 V2M2048dt0001EXACT88;
```

```
%%%%%%%%%%%%%%%%%Time Tests for V=1, M=512 %%%%%%%%%%%%%%%%%%%%%%%%%%%%%%%%

V2M512dt0188 = gpesolve(8,512,1,.01,1,1,2);
save V2M512dt0188 V2M512dt0188;

V2M512dt00588 = gpesolve(8,512,1,.005,1,1,2);
save V2M512dt00588 V2M512dt00588;

V2M512dt002588 = gpesolve(8,512,1,.0025,1,1,2);
save V2M512dt002588 V2M512dt002588;

V2M512dt0012588 = gpesolve(8,512,1,.00125,1,1,2);
save V2M512dt0012588 V2M512dt0012588;

V2M512dt00062588 = gpesolve(8,512,1,.000625,1,1,2);
save V2M512dt00062588 V2M512dt00062588;

V2M512dt000001EXACT88 = gpesolve(8,512,1,.000001,1,1,2);
save V2M512dt000001EXACT88 V2M512dt000001EXACT88;

%%%%%%%%%% Spatialization Error Tests V=0 t=1,dt=.0001 %%%%%%%%%%
V0M32dt000116 = gpesolve(16,32,1,.0001,1,1,0);
save V0M32dt000116 V0M32dt000116;

V0M64dt000116 = gpesolve(16,64,1,.0001,1,1,0);
```

```
save V0M64dt000116 V0M64dt000116;

V0M128dt000116 = gpesolve(16,128,1,.0001,1,1,0);
save V0M128dt000116 V0M128dt000116;

V0M256dt000116 = gpesolve(16,256,1,.0001,1,1,0);
save V0M256dt000116 V0M256dt000116;

V0M512dt000116 = gpesolve(16,512,1,.0001,1,1,0);
save V0M512dt000116 V0M512dt000116;

V0M2048dt000001EXACT16 = gpesolve(16,2048,1,.0001,1,1,0);
save V0M2048dt000001EXACT16 V0M2048dt000001EXACT16;

%%%%%%%%%%%%%%%%%%Time Tests for V=0, M=512 %%%%%%%%%%%%%%%%%%%%%%%%%%%%%%%%

V0M512dt0116 = gpesolve(16,512,1,.01,1,1,0);
save V0M512dt0116 V0M512dt0116;

V0M512dt00516 = gpesolve(16,512,1,.005,1,1,0);
save V0M512dt00516 V0M512dt00516;

V0M512dt002516 = gpesolve(16,512,1,.0025,1,1,0);
save V0M512dt002516 V0M512dt002516;

V0M512dt0012516 = gpesolve(16,512,1,.00125,1,1,0);
```

```
save V0M512dt0012516 V0M512dt0012516;

V0M512dt00062516 = gpesolve(16,512,1,.000625,1,1,0);
save V0M512dt00062516 V0M512dt00062516;

V0M512dt000001EXACT16 = gpesolve(16,512,1,.000001,1,1,0);
save V0M512dt000001EXACT16 V0M512dt000001EXACT16;


%%%%%%%%%% Spatialization Error Tests V=1 t=1,dt=.0001 %%%%%%%%%%
V1M32dt000116 = gpesolve(8,32,1,.0001,1,1,1);
save V1M32dt000116 V1M32dt000116;

V1M64dt000116 = gpesolve(16,64,1,.0001,1,1,1);
save V1M64dt000116 V1M64dt000116;

V1M128dt000116 = gpesolve(16,128,1,.0001,1,1,1);
save V1M128dt000116 V1M128dt000116;

V1M256dt000116 = gpesolve(16,256,1,.0001,1,1,1);
save V1M256dt000116 V1M256dt000116;

V1M512dt000116 = gpesolve(16,512,1,.0001,1,1,1);
save V1M512dt000116 V1M512dt000116;

V1M2048dt000001EXACT16 = gpesolve(16,2048,1,.0001,1,1,1);
```

```
save V1M2048dt000001EXACT16 V1M2048dt000001EXACT16;

%%%%%%%%%%%%%%%%%%Time Tests for V=1, M=512 %%%%%%%%%%%%%%%%%%%%%%%%%%%%%%%%

V1M512dt0116 = gpesolve(16,512,1,.01,1,1,1);
save V1M512dt0116 V1M512dt0116;

V1M512dt00516 = gpesolve(16,512,1,.005,1,1,1);
save V1M512dt00516 V1M512dt00516;

V1M512dt002516 = gpesolve(16,512,1,.0025,1,1,1);
save V1M512dt002516 V1M512dt002516;

V1M512dt0012516 = gpesolve(16,512,1,.00125,1,1,1);
save V1M512dt0012516 V1M512dt0012516;

V1M512dt00062516 = gpesolve(16,512,1,.000625,1,1,1);
save V1M512dt00062516 V1M512dt00062516;

V1M512dt000001EXACT16 = gpesolve(16,512,1,.000001,1,1,1);
save V1M512dt000001EXACT16 V1M512dt000001EXACT16;
```

Appendix D

CHANGE OF MATRIX FOR COMPUTING NORMS

In order to compute the error, the norm must be calculated and this can only be done if the matrices being compared have the same dimensions. The method I used to compare the "exact" matrix with it's estimate when those matrices were of different dimensions was to compare the corresponding parts of the exact matrix with their smaller counterparts which is straightforward since all dimensions were powers of 2.

For example, if:

$$\psi_{approx} = \begin{pmatrix} 1 & 4 \\ 2 & 8 \end{pmatrix} \quad \psi_{approx} = \begin{pmatrix} \textcircled{1} & 4 & \textcircled{3} & 7 \\ 2 & 6 & 8 & 1 \\ \textcircled{1} & 4 & \textcircled{3} & 6 \\ 2 & 4 & 4 & 2 \end{pmatrix}$$

then the norm to be calculated would be

$$\left\| \begin{pmatrix} 1 & 4 \\ 2 & 8 \end{pmatrix} - \begin{pmatrix} 1 & 3 \\ 1 & 3 \end{pmatrix} \right\|_{l_2}$$

```
function exact = changeexact(Exact,estimate)
[~,mex]=size(Exact);
[~,m]=size(estimate);
exact = zeros(m);
for i=0:m-1
    for j=0:m-1
        exact(i+1,j+1)=Exact(i*2^(log2(mex)-log2(m))+1,j*2^(log2(mex)-log2(m)
    end
end
```

BIBLIOGRAPHY

[1] *GPELab*, www.iecn.u-nancy.fl/~duboscq/GPELab_about.html, accessed on 05/12/2013.

[2] Mike H Anderson, Jason R Ensher, Michael R Matthews, Carl E Wieman, Eric A Cornell, et al., *Observation of bose-einstein condensation in a dilute atomic vapor*, science **269** (1995), no. 5221, 198–201.

[3] Weizhu Bao, Dieter Jaksch, and Peter A. Markowich, *Numerical solution of the gross-pitaevskii equation for bose-einstein condensation*, Journal of Computational Physics **187** (2003), no. 1, 318 – 342.

[4] Weizhu Bao, Shi Jin, and Peter A Markowich, *On time-splitting spectral approximations for the schrödinger equation in the semiclassical regime*, Journal of Computational Physics **175** (2002), no. 2, 487–524.

[5] Weizhu Bao and Jie Shen, *A fourth-order time-splitting laguerre–hermite pseudospectral method for bose–einstein condensates*, SIAM Journal on Scientific Computing **26** (2005), no. 6, 2010–2028.

[6] Gordon Baym and CJ Pethick, *Ground-state properties of magnetically trapped bose-condensed rubidium gas*, Physical review letters **76** (1996), no. 1, 6–9.

[7] Satyendra Nath Bose, *Wärmegleichgewicht im strahlungsfeld bei anwesenheit von materie*, Zeitschrift für Physik A Hadrons and Nuclei **27** (1924), no. 1, 384–393.

[8] KB Davis, M-O Mewes, MR van Andrews, NJ Van Druten, DS Durfee, DM Kurn, and W Ketterle, *Bose-einstein condensation in a gas of sodium atoms*, Physical Review Letters **75** (1995), no. 22, 3969–3973.

[9] Allan Griffin, David W Snoke, and Sandro Stringari, *Bose-einstein condensation*, Cambridge University Press, 1996.

[10] DAW Hutchinson, E Zaremba, and A Griffin, *Finite temperature excitations of a trapped bose gas*, Physical review letters **78** (1997), no. 10, 1842–1845.

[11] DS Jin, JR Ensher, MR Matthews, CE Wieman, and EA Cornell, *Collective excitations of a bose-einstein condensate in a dilute gas*, Physical review letters **77** (1996), no. 3, 420–423.

[12] Peter D Lax and Burton Wendroff, *Difference schemes for hyperbolic equations with high order of accuracy*, Communications on Pure and Applied Mathematics **17** (1964), no. 3, 381–398.

[13] F London, *The-phenomenon of liquid helium and the bose-einstein degeneracy*, Nature **141** (1938), no. 3571, 643–644.

[14] Christian Lubich, *On splitting methods for schrödinger-poisson and cubic nonlinear schrödinger equations*, Mathematics of computation **77** (2008), no. 264, 2141–2153.

[15] Joseph E Pasciak, *Spectral and pseudo spectral methods for advection equations*, Mathematics of Computation **35** (1980), 1081–1092.

[16] Christopher J Pethick and Henrik Smith, *Bose-einstein condensation in dilute gases*, Cambridge university press, 2002.

[17] PA Ruprecht, MJ Holland, K Burnett, and Mark Edwards, *Time-dependent solution of the nonlinear schrödinger equation for bose-condensed trapped neutral atoms*, Physical Review A **51** (1995), no. 6, 4704.

[18] Gilbert Strang, *On the construction and comparison of difference schemes*, SIAM Journal on Numerical Analysis **5** (1968), no. 3, 506–517.